ELSEVIER

Available online at www.sciencedirect.com

jmr&t
Journal of Materials Research and Technology

journal homepage: www.elsevier.com/locate/jmrt

Review Article

Systematic study of preparation technology, microstructure characteristics and mechanical behaviors for SiC particle-reinforced metal matrix composites

Yunlei Wang [a,*], *Tullio Monetta* [b]

[a] *College of Materials Science and Engineering, Chongqing University of Arts and Sciences, Chongqing 402160, China*
[b] *Department of Chemical Engineering, Materials and Industrial Production, University of Napoli Federico II, Piazzale Tecchio 80, 80125 Napoli, Italy*

ARTICLE INFO

Article history:
Received 7 June 2023
Accepted 16 July 2023
Available online 19 July 2023

Keywords:
Research progress
SiC particle
Metal matrix composites
Microstructure and properties

ABSTRACT

This article provides a review of the research progress on SiC particle-reinforced metal matrix composites (MMCs), which are a novel type of structural material known for their high strength, hardness, and thermal stability. The potential applications of these composites in aerospace, automobiles, electronics, and specialized mechanical equipment are discussed. The article covers the preparation technology, microstructure, mechanical properties, wear resistance, and application of SiC particle-reinforced MMCs. The advantages, disadvantages, and applicability of different methods are compared. Furthermore, this study explores the relationship between the mechanical properties and microstructure of SiC particle-reinforced MMCs. It also examines the influence of interfacial reactions on the macroscopic properties of these materials. Finally, this article summarizes the application of SiC particle-reinforced MMCs in aerospace, automotive, electronics, and other industries. It also discusses the possible future development directions of these materials. These research results serve as a valuable reference for future research and application of SiC particle-reinforced MMCs. Furthermore, they contribute to the advancement of MMC research and development by offering innovative design concepts and research methodologies to create high-quality structural composite materials. Additionally, this research may inspire the proposal of new manufacturing methods to produce composites with enhanced overall performance in the future.

* Corresponding author.
E-mail address: wangyunlei@alu.cqu.edu.cn (Y. Wang).

https://doi.org/10.1016/j.jmrt.2023.07.145

1. Introduction

Due to the exceptional mechanical qualities of particles, including their high strength, high elastic modulus, and good electrical and thermal conductivity, they are one of the most promising reinforcements for MMCs [1–3]. The related particulate matters are listed as carbon nanotubes (CNTs) [4], silicon carbide (SiC) [5], zirconium oxide (ZrO_2) [6], aluminium oxide (Al_2O_3) [7,8], and titanium diboride (TiB_2) [9], among others. Aluminum matrix composites (AMCs), which are a form of MMC, are widely used in various industrial applications due to their high specific modulus, exceptional strength, good wear resistance, and high thermal conductivity [10–12].

Over the last few years, there has been significant interest in the fundamental research and practical use of MMCs strengthened by CNTs and SiC [13–15]. In recent years, the main focus has been on the SiC and nano-sized SiC reinforced MMCs in terms of preparation, microstructure, properties, and strengthening effect. Composite materials are made up of multiple materials that have varying physical and chemical properties [16–19]. When these materials are combined, they create a new material with a range of properties that differ from those of the individual components [20,21]. Although composite materials are heterogeneous at a microscopic level, they appear homogeneous at a macroscopic level. Typically, a MMC consists of two components: a matrix and reinforcement [22]. These materials are combined in a way that maximizes their benefits while minimizing their drawbacks.

The process of casting in liquid form allows for the creation of items with intricate designs [23]. It would be desirable to create lightweight bulk parts made of metal matrix nanocomposites (MMNCs) that have an even distribution of reinforcement and maintain structural integrity. However, the use of nano-sized ceramic particles presents challenges due to their high viscosity, low wettability in metal matrices, and large surface area-to-volume ratio. Achieving a uniform dispersion of these particles in liquid metals is difficult. To address this issue, pretreatment of the particles is necessary to enhance their ability to bond with the metal matrix [24,25].

In previous research, it was found that numerous scholars have conducted successful experiments and synthesized products with outstanding performance [26,27]. The microstructure and mechanical properties of SiC/Al composites were investigated through scanning electron microscopy and tensile tests to analyze the observed trends. The results indicated that the mechanical properties of the composites are significantly affected by the uniformity of the distribution of SiC particles [28]. The corrosion performance of SiC/Al composites was studied by Karthikraja [29] in various acidic and alkaline conditions. The findings indicated that these composites, which consist of SiC particles embedded in an aluminum matrix, exhibit a strong resistance to corrosion. Additionally, the researchers examined the thermal stability of SiC/Al composites in high-temperature settings [30]. The findings indicated that SiC/Al composites exhibit favorable stability at elevated temperatures. The article discusses the utilization of these composites in the aerospace industry, specifically for producing aero-engine components and structural materials for aircraft [31].

The aim of the study was to examine the impact of the microstructure of the matrix, as well as the size, shape, and distribution of the reinforcement phase, on the tensile properties of MMCs that contain particles. This was accomplished through both experimental and numerical analysis of the deformation characteristics [32]. The study conducted by Ozdemir et al. [33] examined various aspects, including the distribution of reinforcement and intermetallic phases, porosity levels, microstructure of the matrix phase, interfacial condition, and mechanical characteristics. Yigezu et al. [34] conducted a study comparing the microstructures and mechanical properties of Al-4% Cu-2.5% Mg matrix composites reinforced with 5 wt% SiC and Al_2O_3 particulates. The study examined the yield strength, ultimate tensile strength, elastic modulus, percentage elongation, hardness, percentage porosity, and fracture characteristics. The study of [35] examined the impact of Zr inclusion on the wear characteristics and microstructure of AMCs that were reinforced with B_4C and SiC particles. These composites were produced through hot pressing. The mechanical behavior of metal-matrix composites made of SiC/Al was analyzed using 2D micromechanical analysis under various types of loads, including tensile, shear, and combined tensile/shear loads. The study investigated the impact of interface strength and loading conditions on the composites [36]. To investigate the impact of particle arrangements, interface strengths, and loading conditions on the stiffness and strength properties of the composite, a series of computational experiments were performed on the representative volume element (RVE). The study [37] focused on the production and analysis of aluminum matrix composites reinforced with SiC and Si_3N_4. The main objective was to identify the key factors that influence and improve the tribological performance of the composites. The results showed that increasing the percentage of Si_3N_4 reinforcement had a moderate effect on reducing the wear rate of the composites. The authors of a study, Upadhyay et al. [38], who described the creation of a Silicon–Boron ($Si_{96}B_4$) alloy using readily available materials and a simple, one-step process called spark plasma sintering. The alloy's improved validity value is attributed to a decrease in thermal conductivity caused by the presence of nanoscale SiC particles and mesoscale SiB_3 precipitates, which scatter heat-carrying phonons. The low cost and non-toxic nature of the constituent elements, along with the ease and scalability of the synthesis process, suggest that $Si_{96}B_4$/SiC nanocomposites could be a promising p-type thermoelectric material for high-temperature power generation applications.

The modern world has shown a technological interest in developing techniques to create high-performance MMCs that are reinforced with lightweight aluminum particles. This is due to the demand for such composites in various sectors, including aerospace, defense, and industrial, where superior mechanical properties are required [39]. The study conducted by Guttikonda et al. [40] focused on examining the impact of changes in microwave processing temperatures on the microstructural and mechanical characteristics of a hybrid composite made from AA7075, SiC, and graphite using powder metallurgy methods. The researchers used hybrid microwave sintering techniques to create a composite material that has a strong and flawless bond between the matrix and reinforcement particles. The microwave-sintered nano-hybrid composite had a significantly higher strain-to-fracture value of 12.24% compared to the conventional sintered composite, which had a value of 6.12%. To assess the hot workability of the multi-size SiC particle-reinforced 6013 AMCs, the researchers examined the hot deformation behavior, constitutive model, processing map, and microstructure using a scanning electron microscope (SEM) in studies [41–43].

Despite decades of research and significant investment in particle-reinforced AMCs, their current level of application and created value is not proportional. This is due to limitations in their application and the absence of commercialized production processes. To address this issue, there is an urgent need for research and application of composites. The focus should be on developing low-cost casting products and producing a range of products with different properties to meet various application needs. This approach will facilitate large-scale industrial production [44,45]. In the past two or three decades, numerous scholars both domestically and internationally have dedicated their efforts to researching particle-reinforced aluminum matrix composites. They have made significant advancements in the development of SiC_p/Al composites for high-performance structural components used in aircraft, missiles, and engines. So far, the SiC_p/Al particle has been developed with various techniques for preparing SiC_p/Al composites. These techniques include stirring casting [20], powder metallurgy [46], wrapping, hot extrusion, spray deposition [47], semi-solid-vortex, and high-energy ultrasonic semi-solid composite process, among others. This article provides an overview of various methods used to prepare composites consisting of an aluminum matrix reinforced with SiC. The advantages and disadvantages of each method are analyzed, and potential future trends in composite preparation and application are discussed [20,22]. Overall, these composites have great potential for use in various economic sectors and have attracted significant attention. Moving forward, there will be a focus on developing aluminum matrix composites and allocating financial and material resources to relevant institutions, universities, and companies.

2. Preparation technology

In this paper, several common preparation processes of SiC reinforced MMCs are introduced [20,46,47]. The preparation process and related equipment are described, and the changes in microstructure and properties of the composites are summarized. In order to propose appropriate research ideas for scientific and technological professionals, it is important for them to be familiar with this research method. This will ultimately enable them to contribute more effectively to the development of relevant composite materials and their application in engineering practice in the future.

As far as we know, it is mainly divided into a common preparation process and some relatively novel preparation methods. The commonly used preparation methods include ball milling, stir casting, squeeze casting, liquid metal infiltration, powder metallurgy, spark plasma sintering, and spray deposition. The novel preparation methods include in-situ reaction synthesis, mechanical alloying, and high-energy ultrasonic-assisted preparation. Each of these preparation methods has its own advantages and disadvantages. The prepared composite materials also have their own characteristics. However, the common characteristic is that the final performance of particle-reinforced metal matrix composites is relatively excellent [13,26,27].

2.1. *Some common preparation processes*

2.1.1. *Stir casting*

The stir casting process involves adding the reinforced phase to the liquid metal, mixing the liquid and solid phases evenly using a high-speed rotating mechanical stirring device [20], and then pouring the mixture into ingots. The key to this method is that the reinforcing phase is uniformly distributed in the matrix and that the interface between the matrix and the reinforcing phase is well bonded.

Usually, the stir casting process is divided into the liquid phase stirring method and the liquid-solid two-phase stirring method. Compared to other preparation techniques, the stir casting method has many advantages [48,49]. Such as low manufacturing cost and the ability to easily form complex workpieces. The process equipment is relatively simple and can be adapted for mass production. However, there are still some problems in the stir casting process, such as the easy segregation and reaction of ceramic particles at the interface. Secondly, in non-vacuum stirring casting, it is easy to introduce gas during the stirring process, resulting in the formation of internal pores in the product. Thirdly, the volume fraction of the particle-reinforced phase in the metal matrix composite prepared by this method will be limited to a certain extent.

The schematic diagram of the conventional stir casting process for MMC is shown in Fig. 1. SiC particle-reinforced AMCs are utilized to fabricate high-performance particle-reinforced composites. Special applications of aluminum-based materials in railways and automobiles, particularly as lightweight brake discs for automobiles, aim to achieve weight reduction and wear resistance, thereby enhancing mechanical properties and microstructure. An important substantive issue must be addressed: the research on key technologies for the controllable production of SiC particle reinforced AMCs. During the manufacturing process, SiC particles are added to the aluminum liquid through high-speed mechanical stirring. This method prevents the segregation of SiC particles caused by the different specific gravity of the aluminum liquid and enhances the permeability of the SiC particles and the surface of the aluminum liquid. Additionally, the study aims to discuss the number, size, and distribution of SiC particles in the matrix, as well as research the mechanism of enhancing the strength of aluminum matrix composites through the addition of SiC particles [20].

The particles prepared by this method exhibit good wettability and a uniform distribution within the aluminum matrix. The preparation equipment is simple, the cost is low, and it can be used for large-scale production [50]. Now, the mature semi-solid stirring casting method is mainly used for micron particles. However, for sub-micron and nano particles, controlling their uniform distribution in liquid aluminum remains challenging with the stirring casting method. At the

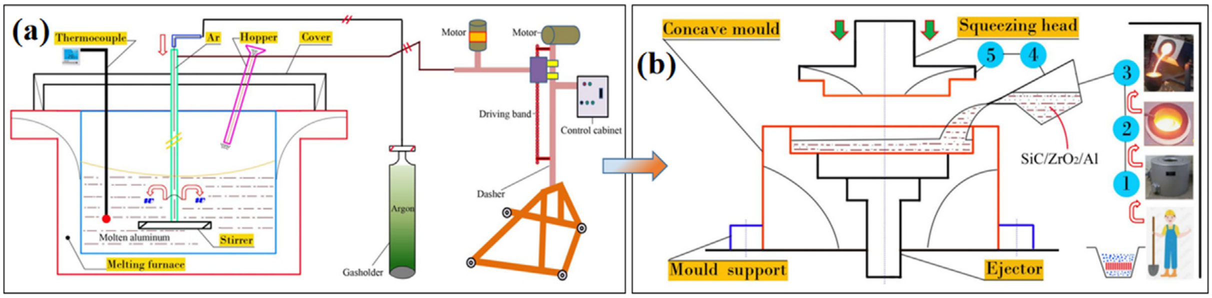

Fig. 1 – Schematic representation of stir casting for MMC (a) smelting process, (b) die casting process.

same time, when the molten metal is in a semi-solid state, its viscosity is relatively high, and it is prone to agglomeration. This can result in a decrease in the composite's related properties.

2.1.2. *Squeeze casting*

The Al 6082/SiC_p composite was created through a squeeze casting process [51], which involved adding SiC particles to the 6082 matrix. Fig. 2 displays a diagram of the equipment used for fabrication. The process for preparing the composite is outlined in detail below.

To obtain a pure melt, the 6082 aluminum ingot is first cut into blocks and then polished with sandpaper to remove the oxide layer. The blocks are then placed in a steel crucible and heated to 780 °C using a crucible resistance furnace. Argon gas is introduced into the molten aluminum alloy to degas and refine it. The temperature of the molten metal is then controlled at 730 °C.

A stirring head made of steel and equipped with four blades was heated to 200 °C and coated with ZnO. It was then attached to a stirrer and placed in a liquid alloy. SiC pellets were treated in an annealing oven at 1000 °C for 2 h to create a SiO_2 film and improve the wettability between the pellets and the aluminum liquid. The pellets were then dried at 300 °C before being added to the molten metal. The stirring speed was set at 350 rpm, and the SiC particles had an average feed rate of 4 g/min. The 6082 aluminum alloy was mixed with 3 wt % of SiC particles. Stirring continued at the same speed for 5 min, and argon gas was used to prevent oxidation of the molten aluminum during the process. This is illustrated in Fig. 2(a).

Fig. 2(b) displays a diagram of the extrusion casting process. Molten metal, with and without SiC particles, was poured into a preheated conical steel die at a temperature of 200 °C. The die had dimensions of 30 mm on the longer side, 28 mm on the shorter side, and 90 mm on the higher side. The extrusion process was conducted using an extrusion pressure of 50 MPa and a holding time of 1 min. Afterward, the solidified sample was removed. To compare the microstructure and properties of squeeze casting and permanent mold casting (PMC), the same molten metal was poured into a steel mold without undergoing the extrusion process [27,35]. All samples underwent a T6 heat treatment, which included a solid solution treatment at 540 °C for 1 h, followed by artificial aging at 180 °C for 8 h.

The main advantages of using the squeeze casting are: (1) low preparation costs, (2) the shape of the parts made is the same or similar to the final part, and (3) it can reduce the interfacial reaction between the particles. However, there are certain difficulties in manufacturing parts with complex

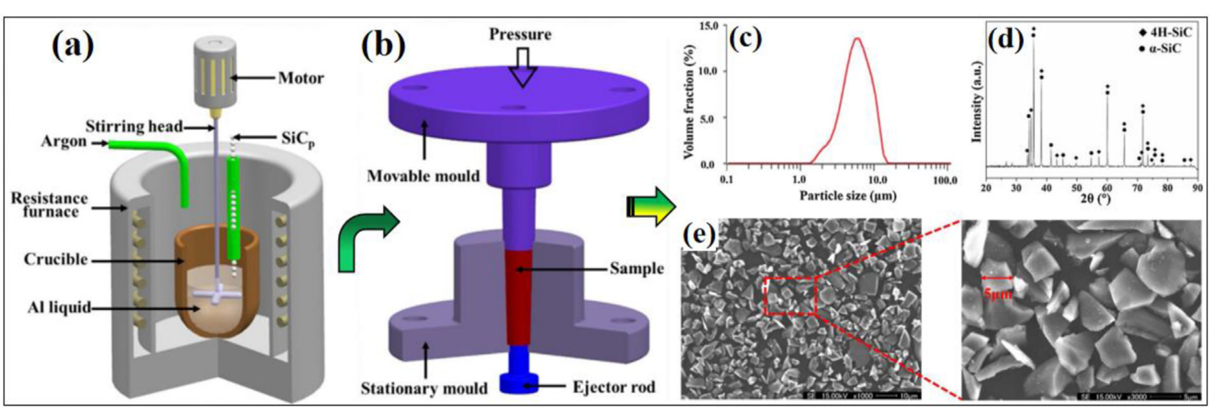

Fig. 2 – (a-b) The sketch of fabrication of the SiC_p/Al 6082 composites via squeeze casting; (c) SiC_p particle size; (d) XRD pattern; (e) morphology [51].

shapes, and the relatively high pressure applied by squeeze casting is limited to some extent [51].

2.1.3. Deformation-driven metallurgy

A composite material with a diameter of 16 mm and a height of 1 mm was produced using deformation-driven metallurgy (DDM) process [52]. The process took 30 s and involved a rotation speed of 1200 rpm. The process is illustrated in Fig. 3.

This is a typical method for preparing SiC composites, which combines ball milling and pressure deformation. The prepared SiC/AMCs have a uniform microstructure and good material properties. Therefore, it can be widely used in structural devices. A planetary ball milling device (QM-3SP2, Nanjing University Instrument Plant) was used to mix the SiC/Al powders. The ball-to-powder ratio, milling time, and rotation velocity were 200 rpm, 10 h, and 5:1, respectively. The ZrO_2 milling balls have a diameter of 6 mm. Both micro-SiC and nano-SiC particles, especially the nano-SiC particles that tend to aggregate easily, were consistently mixed with Al powders, as shown in Fig. 3(a and b). It was possible to create sound nano-SiC reinforced AMCs (SiCnp/AMCs) because the surface of Al powders was uniformly covered by nano-SiC particles (see Fig. 3(a)).

2.1.4. Spray deposition

Fig. 4(a) is a schematic diagram of the process for cold spray deposition of Al matrix composites using two powder feed lines [53]. By using a constant powder feed rate (5 rpm) and a range of SiC powder feed rates (i.e., from 0 to 3 rpm), different microstructural configurations can be obtained within the deposited layer, the pure Al deposition homogeneous bonding (Al-SiC_p) in b_0, b_1, b_2 and b_3, and hierarchical bonding in $b_{0\text{-}3}$.

A promising method for coating surfaces with various nanoparticles and chemicals, while accurately controlling the microstructure of the deposition, is ultrasonic spraying. The schematic diagram of the spraying procedure and the spraying path is shown in Fig. 4(b). Each sample underwent a total of 12 passes at a nozzle velocity of 10 mm/s. The spray area overlapped, and the final deposited structure was uniform, thanks to the small separation of 2 mm between the centers of two adjacent lines. Finally, the AZ31/SiC composite material was prepared [49].

In this method, several processing factors, which can be categorized into two groups-suspension and spraying parameters, may affect the structure of the spray-deposited material. The parameters of the suspension include the type, size, and concentration of suspended particles of SiC. For two distinct particle sizes of 80 and 800 nm, the effect on the surface tension was investigated using suspension concentrations of 0~16 wt% SiC [54]. Due to the particles' tendency to settle and clog spraying tubes and equipment, maintaining homogeneity in the suspension of the 800 nm SiC during the spraying operation was challenging. However, the suspension of 80 nm SiC particles could be maintained in a stable state for days, which was advantageous for the spraying procedure.

This method is a novel preparation process for aluminum matrix composites. It aims to reduce the interface reaction between the reinforcement particles and the matrix, promote grain refinement and uniform distribution, simplify the process, shorten the production cycle, and reduce production costs. However, the utilization rate of particles is low.

2.1.5. Powder metallurgy

Fig. 5(a) depicts the steps involved in making a composite of $Mg_2(Si_{04}Sn_{0.6})Sb_{0.015}/(y)SiC$ [55]. The first and most crucial step in the entire material preparation process is the vacuum induction levitation melting (IM) process. The bulk materials used in this method were Mg (99.9 wt%), Si (99.9 wt%), and Sn (99.9 wt%). They were placed in an alumina crucible with graphite carbon paper before being transferred to a water-cooled copper crucible. This process produced $Mg_2Si_{04}Sn_{0.6}$ melted ingots under a vacuum of 101 Pa. To compensate for the loss caused by volatilization in the IM process, there was a 10 wt% excess of magnesium. The output power, time, and melting times for this method are 14~17 kW, 80–100 s, and 3 times, respectively. In the MA process, the as-melted ingots were combined with doped Sb (99.99 wt%) and nanocomposite SiC (99.9 wt%) powders with the chemical formula

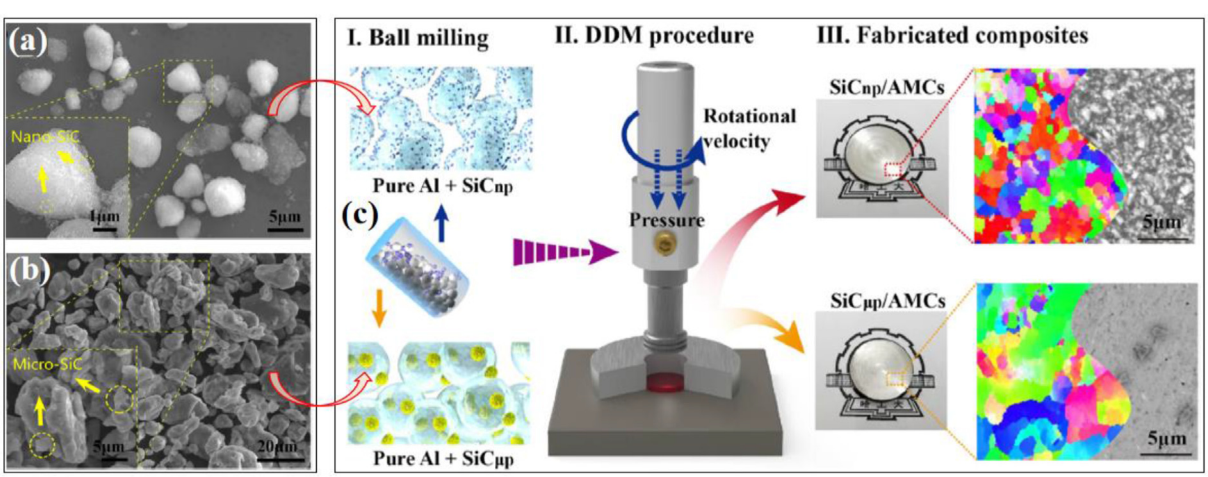

Fig. 3 – (a-b) Microstructure of SiC for ball-milled, (c) schematic of deformation-driven metallurgy procedure [52].

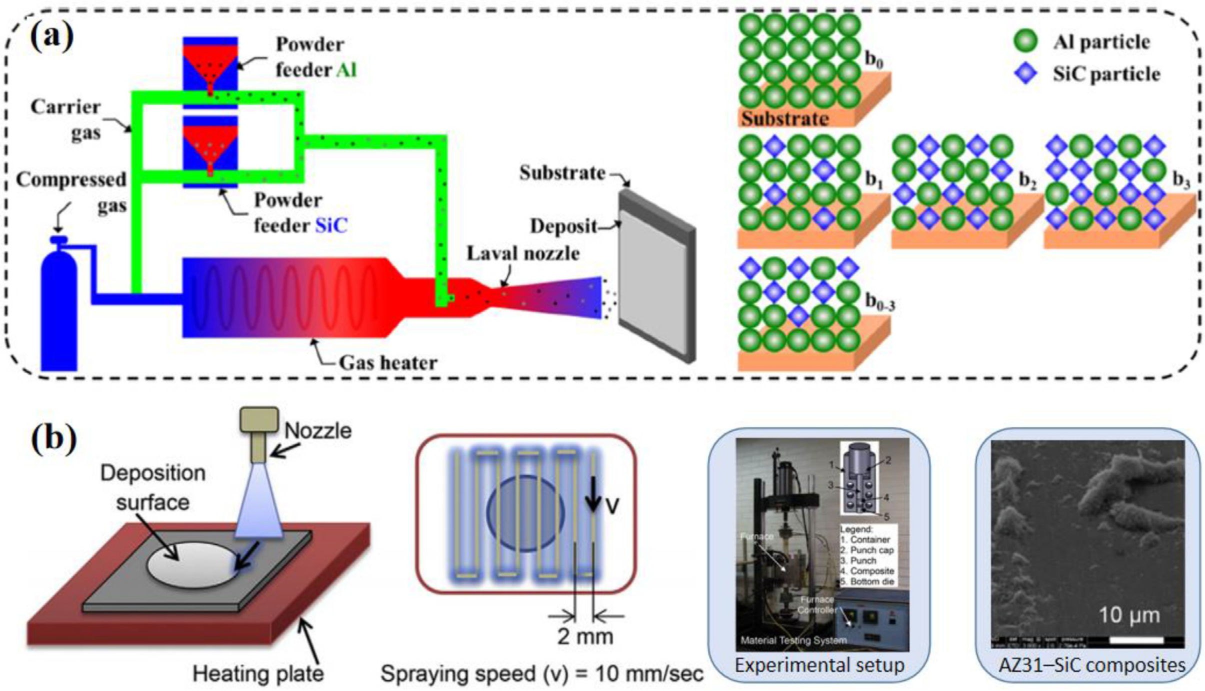

Fig. 4 – Schematic illustrations of (a) the cold spray deposition of SiC/Al composites [53], (b) spray deposition process of AZ31-SiC composites [54].

$Mg_2(Si_{0.4}Sn_{0.6})Sb_{0.015}$/(y)SiC in a ball mill tank under an argon environment to create a mixed powder. The MA process used a self-built high-energy ball mill with balls made of WC-cemented carbide and a tank made of the same material. Ball mills are typically operated in dry milling mode with a fixed ball-to-material ratio of 10:1 and a rotational speed of 400 r/min. The milled powder was placed into a graphite mold with a 20 mm diameter under vacuum conditions (10^{-1} Pa) SPS processing to produce samples of $Mg_2(Si_{0.4}Sn_{0.6})Sb_{0.015}$/(y)SiC.

The sample assembly in the spark plasma sintering furnace and shear test for the composite of C_f/SiC/$AlCoCrFeNi_{2.1}$ [56], which is shown in Fig. 5(b). Finally, C_f/SiC composites were successfully joined using an $AlCoCrFeNi_{2.1}$ eutectic high-entropy alloy filler via SPS technology, resulting in a uniform microstructure and excellent mechanical properties.

Powder metallurgy is the earliest developed process for preparing particle-reinforced metal matrix composites. It involves the screening and uniform mixing of metal powder and reinforced ceramic particles, followed by cold pressure consolidation, degassing, sintering, and subsequent treatment to produce composite materials. Fig. 6 shows the conventional process of preparing SiC-reinforced aluminum matrix composites through powder metallurgy [57]. Hot extrusion of sintered samples can reduce the number of voids, refine grains, improve the interfacial bonding strength of

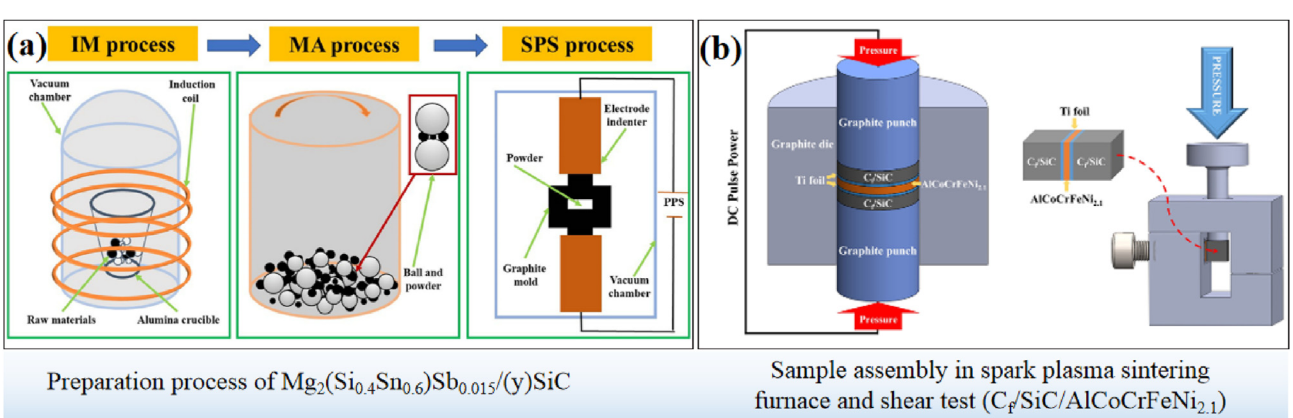

Fig. 5 – The preparation process via spark plasma sintering of (a) $Mg_2(Si_{0.4}Sn_{0.6})Sb_{0.015}$/(y)SiC [55], (b) sample assembly in spark plasma sintering furnace and shear test (C_f/SiC/$AlCoCrFeNi_{2.1}$) [56].

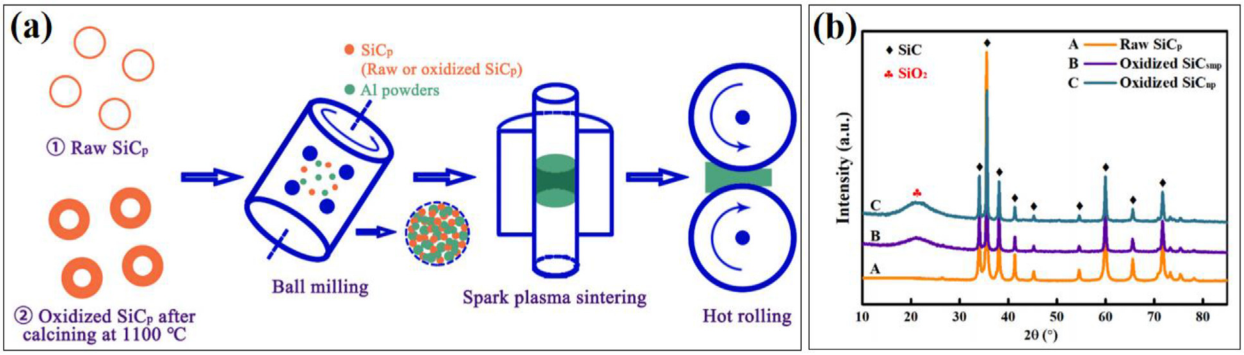

Fig. 6 – (a) Fabrication process of SiC_p/Al composites by powder metallurgy, (b) XRD patterns of SiC_p before and after calcining [57].

composites, and enhance the distribution of SiC particles. This process effectively improves the mechanical properties of the composites. After undergoing heat treatment, such as solution, quenching, and aging, the mechanical properties of the composites can be further enhanced.

The advantages of the powder metallurgy method are that it allows for the easy preparation of metal matrix composites with a high content of strengthening phase. It also enables better control over the uniformity of particle distribution in the matrix. Additionally, the metal matrix composites prepared using this method exhibit more stable performance indexes compared to other methods. In addition, compared to the same material produced by the molten metal process, the particle-reinforced aluminum matrix composite prepared by the powder metallurgy process exhibits higher strength levels and improved microstructure. However, the process and equipment involved in this method are more complex. Incomplete degassing can result in the formation of pores in the material, and improper temperature selection can easily lead to segregation. In addition, it is difficult to produce parts of the desired size using this method, making it unsuitable for the production of large-sized parts. Therefore, it is not suitable for the mass production of aluminum matrix composites [45].

SiC_p/Al composites are produced using a powder metallurgy technique illustrated in Fig. 6(a). As raw materials, spherical pure Al powders (99.95% purity), raw SiC_{smp}, and raw SiC_{np} were employed [57]. Spherical Al powders have a diameter of around 25 μm, while raw SiC_{smp} and raw SiC_{np} have diameters of about 40 nm and 700 nm, respectively. And the XRD patterns of SiC_p before and after calcining are shown in Fig. 6(b). The XRD patterns also support the development of SiO_2 layers. After calcining at 1100 °C, the distinctive SiO_2 peak could be observed in the XRD patterns of both SiC_{smp} and SiC_{np}. Amorphous SiO_2 was difficult to fully crystallize at 1100 °C due to the presence of additional amorphous components, which is the primary reason for the broader characteristic peak of SiO_2.

However, powder metallurgy also has some drawbacks, such as high costs, a complicated process, and long production cycles. However, powder metallurgy is currently evolving towards achieving high densification, high performance, integration, and low cost. With the deepening of research, the application scope of powder metallurgy will become more extensive.

2.2. *Some novel preparation methods*

2.2.1. *In-situ reaction synthesis*

The basic principle of in-situ reaction synthesis technology is to select the appropriate reaction agent according to the design requirements and carry out a biochemical reaction at the appropriate temperature. This process results in the in-situ generation of one or several types of matrix with high melting point, high hardness, and high elastic modulus, thereby strengthening the metal matrix. Most of the reinforcements are autogenous ceramic particles, including SiC, TiC, AlN, Al_2O_3 and TiB_2. These particles have a stronger affinity compared to external ceramic particles and can effectively reduce the agglomeration and segregation of the reinforcements [58].

It is widely recognized that the properties of MMCs are influenced by the size and volume fraction of the reinforcements, as well as the nature of the matrix-reinforcement interfaces. An optimal set of mechanical properties can be achieved when fine and thermally stable ceramic particles are uniformly dispersed in the metal matrix. Efforts have been made to meet these requirements. The work has led to the development of novel composites, specifically in situ MMCs, where the reinforcements are synthesized within a metallic matrix through chemical reactions between elements or between an element and a compound during the fabrication process. Compared to conventional MMCs produced by ex situ methods, in situ MMCs offer several advantages: (a) the reinforcements formed in situ are thermodynamically stable within the matrix, resulting in reduced degradation at high temperatures; (b) the interfaces between the reinforcement and matrix are clean, leading to strong interfacial bonding; (c) the in situ formed reinforcing particles are smaller in size and more uniformly distributed within the matrix, resulting in improved mechanical properties.

Fig. 7 illustrates the timeline of microstructure changes during the heating process [58]. Initially, a thin layer of oxidation forms on the surface of the alloy, which gradually

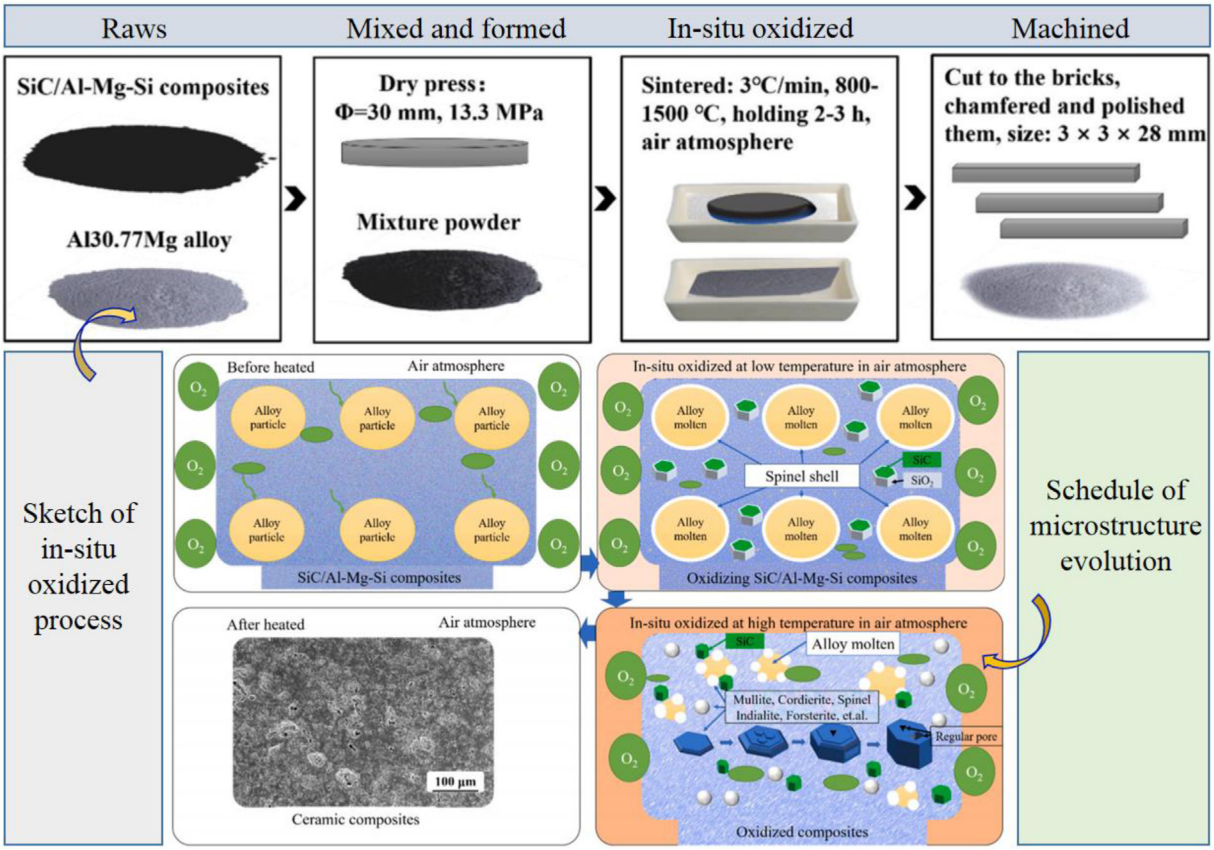

Fig. 7 – The sketch of synthesized composites by in-situ oxidized process and microstructure evolution in the heating process [58].

thickens as the temperature and heating time increase. The molten alloy tends to form spheres or flow into pores due to surface tension and gravity. This causes the dense oxide layer to crack and react with oxygen and ceramic grains, forming Spinel, Mullite, and Cordierite. The addition of alloy increases the liquid phase, which leads to the agglomeration of tiny particles. Additionally, the increased amount of alloy accelerates the oxidizing process of SiC through the dissolved oxidized shell, providing enough Si to produce Mullite, Cordierite, and Indialite phases.

In-situ reaction synthesis is a recently developed process for preparing composite materials. This method is based on the reaction between elements in the aluminum matrix or between elements and compounds to produce one or more reinforced particles. The reinforced particles nucleate from the matrix and grow with excellent thermodynamic stability. Furthermore, the particles produced are well distributed and small at the reaction interface. This method enables the production of high-performance aluminum-based composite materials. This method can produce good performance in particle-reinforced aluminum-based composite materials.

2.2.2. *Mechanical alloying*

Mechanical alloying (MA) has become an important method for preparing nanocomposites with excellent properties. It involves mechanical mixing, dispersion strengthening, self-propagating sintering, and in-situ reaction synthesis [59]. The interface is free from impurities and has a strong bonding strength.

Because there is a significant difference in particle size between the reinforcement particles and the matrix powder, it is not possible to achieve uniform mixing using the ordinary mechanical mixing process for sub-micron reinforced particles and matrix powder that differ by dozens of microns. Most of the reinforcing particles in the composite powder are in the sub-micron range. The smaller the particle size, the better the distribution uniformity. In the ball milling process, the fine oxide particles are crushed and then incorporated as a second phase reinforcement, resulting in an even distribution within the aluminum alloy matrix. This further enhances the mechanical properties of the material.

The traditional powder metallurgy process was used to create the Cu-based powder metallurgy brake pads. The majority of the electrolytic Cu, Sn, Ni, W, graphite, reduced Fe, h-BN, and produced composite ceramic powder (B_4C–SiC) were chosen as the raw materials. According to Fig. 8(a), the manufacturing procedure for Cu-based powder metallurgy brake pads can be divided into three parts. The powders were first placed into the V-shaped mixer for 9 h with a small amount of aviation kerosene. Then, the combined powders were pressed into green compacts using a pressure of 600 MPa for 15 s. The resulting compacts had dimensions of

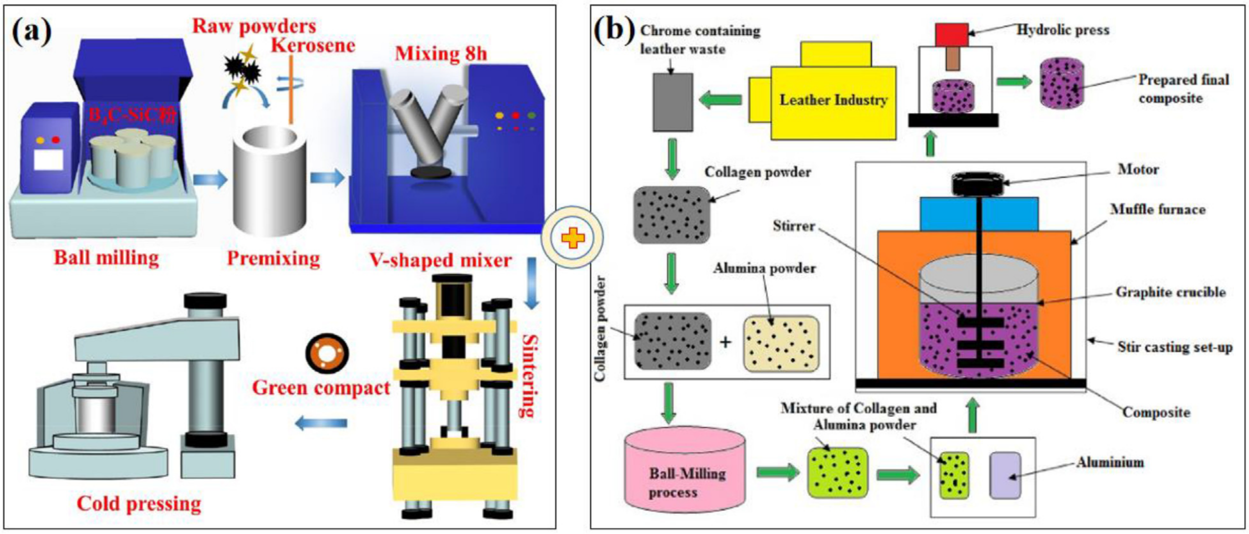

Fig. 8 – (a) Experimental preparation flow chart by ball milling [59], (b) fabrication of hybrid composite material by ball milling [60].

75mm × 53 mm. In the end, Cu-based powder metallurgy brake pads were pressure sintered at 5 MPa and 940 °C for 3 h in a mixed gas environment of N_2 and H_2.

To understand the ball milling process for other composites, refer to the line graph of the stir casting configuration shown in Fig. 8(b). The Al/5 wt% Collagen/5 wt% Al_2O_3 hybrid composite material was placed in the solid-liquid converter in the mushy area to apply squeezing pressure. It was then transferred to a universal testing machine (U.T.M.). To eliminate porosity and shrinkage that occur during the solidification process, pressure was applied using a cylindrical die punch [60].

As we know, ball milling is a mechanical alloying technology used to create a uniform material. In this process, powder particles are fractured and the blended powder pieces are repeatedly cold welded. It is easy to control the size and shape of powder particles using this technique. By blending essential or pre-alloyed particles, solid-state powder processing technology creates various equilibria and nonequilibrium alloying stages. Hybrid composite material is created when the matrix material contains two or more reinforcing components.

2.2.3. *High energy ultrasonic assisted preparation*

Ultrasonic waves are sound waves with frequencies above 20 kHz. When the intensity of an ultrasonic wave exceeds a certain threshold, it can impact or alter the structure and properties of the medium through its interaction with it. This type of ultrasonic wave is referred to as high-energy ultrasound. Nonlinear effects, such as acoustic cavitation and acoustic flow, are generated when high-energy ultrasound propagates through metal or alloy melt. The main functions of high-energy ultrasonic technology are refining grain, creating a uniform microstructure, degassing, and removing slag. This technology is an effective way to improve the solidification microstructure and mechanical properties of metals or alloys. After undergoing high-energy ultrasonic treatment, the alloy's mechanical properties are significantly enhanced. This includes a 10%–30% increase in yield strength, a 20%–40% increase in tensile strength, and a 20%–40% increase in elongation. Furthermore, the forging properties and other hot working properties are greatly improved.

When high-energy ultrasonic technology is used to treat metal or alloy melt, the instantaneous high pressure and high temperature caused by the acoustic cavitation effect can clean and activate the surface energy of particles. This process increases the surface energy of particles and reduces the surface energy of the melt. As a result, it improves the wettability and compatibility between components in a short time and promotes the fusion of particles and melt. The stirring effect of acoustic flow ensures uniform dispersion of particles on a macro level. Additionally, the combined effect of acoustic cavitation and acoustic flow promotes uniform dispersion of particles on a micro level. This results in metal matrix composites with improved interface bonding and enhanced performance. The process of material preparation is not restricted by factors such as particle wettability, uniform dispersion, and particle size, which significantly hinder the widespread adoption of conventional preparation methods.

The ultrasonic-aided rheo-squeeze casting process was conducted using an ultrasonic vibration device, as depicted in Fig. 9. A specific quantity of alloy liquid was poured into a preheated metal cup and then placed inside an insulation furnace. The ultrasonic vibration head was lowered and submerged into the molten material for 15~20 mm. When the melting temperature reached the initial vibration temperature, the ultrasonic vibration was immediately initiated. The temperature range for vibration of A1 and A2 alloys is 650~625 °C and 665~640 °C and the vibration time is 90s. The melt treated with ultrasonic waves was poured into the preheated mold cavity of the extruder, which was at a temperature of approximately 200 °C. The upper and lower buttons were pressed

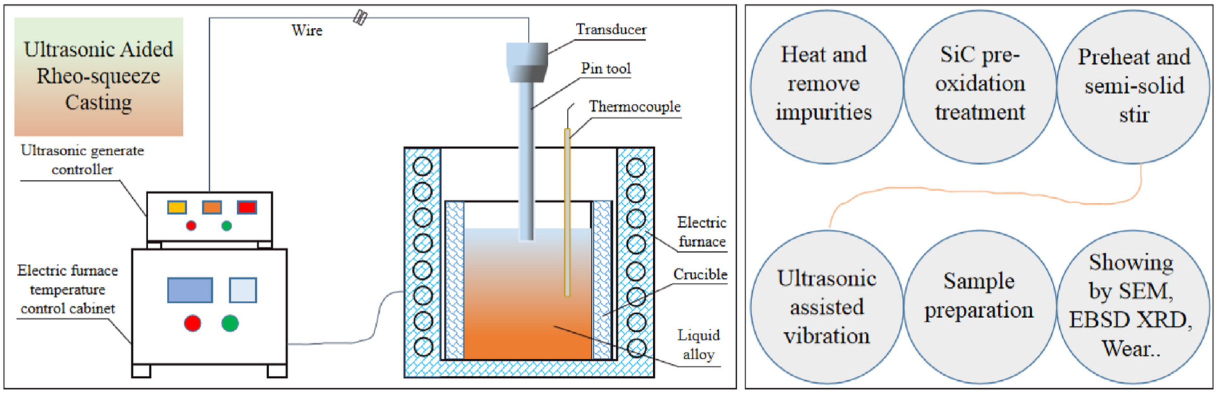

Fig. 9 – Schematic representing the novel fabrication process by ultrasonic aided rheo-squeeze casting.

simultaneously, and the casting was ejected after maintaining pressure for 60 s. The size of the part was 30 mm × 80 mm, and the pressure used was 0, 100, 200, and 300 MPa sequentially. In order to investigate the impact of ultrasonic action on alloy solidification, the aluminum alloy melt without ultrasonic treatment (with the same melting process and melt mass) was directly poured into the extrusion mold cavity at a temperature of 700 °C for comparative analysis.

Through a unique ultrasonic-assisted rheo-squeeze casting process, an Al 6061 alloy reinforced with various combinations of nanoparticles was created [61]. The innovative process produced high-density hybrid ceramics with minimal levels of nanoparticle aggregation, refined grain structure, and reduced porosity. The investigation of the hardness, tensile strength, and wear behavior of the cermets revealed that as the amount of ceramic particles in the Al alloy increased, the mechanical properties of hybrid cermets also increased, along with their corrosion resistance.

2.2.4. *Permanent mold cast and powder thixoforming*

Compare to other research studies, this study aims to describe the benefits of the unique technology and explain how SiC_p strengthens the PTF-SiC_p/6061Al composite. To accomplish this, a series of composite samples were created using powder thixoforming (PTF) [62]. The samples consisted of 6061 Al-based alloy reinforced with 10 vol% of 6.94 μm SiC_p, as depicted in Fig. 10. The microstructure, mechanical characteristics, and fracture behavior resulting from this process were thoroughly examined and compared to those of the matrix alloys made using permanent mold cast (PMC) and PTF, respectively.

To determine the yield strength of this composite, a modified model based on three strengthening mechanisms was presented. The findings from the experiment were found to be highly consistent with the theoretical results obtained.

In general, composites prepared by powder metallurgy have various advantages in terms of process and properties. These include uniform distribution of reinforcement particles, good wettability, and a compact structure. This process has been applied earlier and is relatively mature. The stir casting process has major drawbacks in all areas except for its lower cost. The production is mostly limited to small parts. Squeeze casting and spray deposition processes are positioned between powder metallurgy and stirring casting. On the other hand, in-situ reactive synthesis is a recently developed technology that offers exceptional properties and has a growing range of applications. This technology is continuously evolving and advancing.

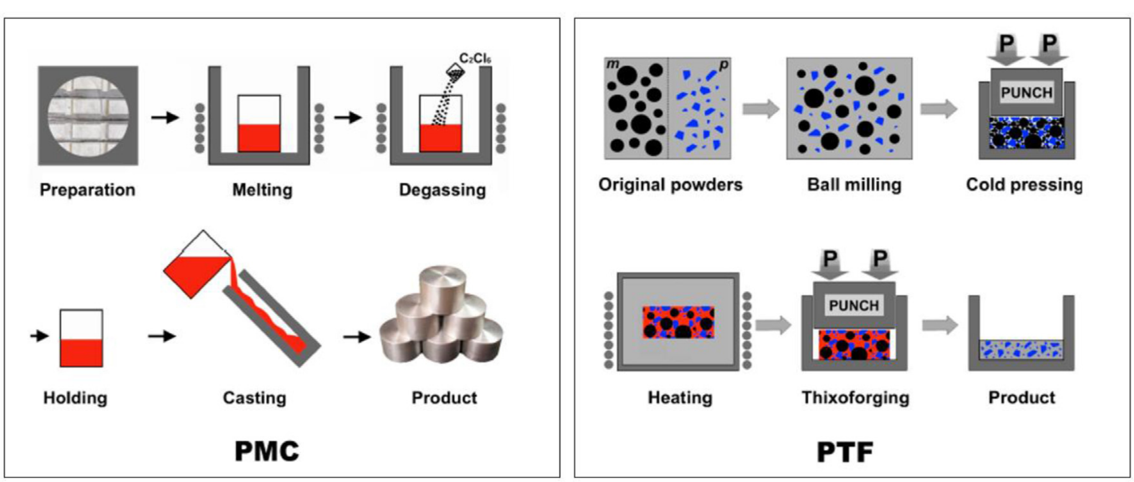

Fig. 10 – Schematic illustration of the PMC and PTF process (m: matrix; p: SiC_p) [62].

3. Microstructure characteristics of composites

3.1. *Microstructure evolution of stirring casting*

As the initial layer of the cladding composite, an aluminum alloy was melted, cast, and formed into a mold. A second layer of molten metal was then poured over the solidified metal layer, creating a composite material for cladding. The fact that the entire procedure is carried out in a vacuum environment ensures that no alumina film forms on the surface of the top layer of the composite materials used for cladding. SiC_p/A356 AMCs melt was produced by stir casting, which offers several advantages in terms of economy, simplicity, and the ability to create large and intricate parts, for the preparation of A356-SiC_p/A356 cladding composite materials.

Under vacuum conditions, the industrial aluminum alloy A365 was melted in a medium frequency induction furnace. The scanning electron microscope (SEM) morphology and particle size of the experimental SiC are shown in Fig. 11(a and b). As the first layer of the cladding composite material, the molten material was poured into a permanent mold. The mold had a bottom diameter of 40 mm, a top diameter of 50 mm, and a height of 100 mm. The material was filtered before being poured. The residual A365 aluminum alloy melt was then mixed with weighed SiC particles at 620 °C to create a 20 wt% SiC_p/A365 composite slurry. Fig. 11(c2) provides micrographs of the SiC_p/A356 layer, the A356 alloy layer, and the interface of the composite material used for cladding. According to Fig. 5(c), the grain size of the A356 alloy is approximately 196.5 μm. The α-Al grains in the layer display a globular morphology, which is a typical characteristic of a semisolid structure. The α-Al grains in the SiC_p/A356 layer still maintained a spherical morphology, as observed in Fig. 11(c1), but their size reduced to approximately 127.9 μm. The presence of numerous SiC particles in the slurry may act as barriers that prevent the formation of α-Al grains during solidification. Additionally, based on the interface lattice misfit theory [64], the SiC particles could act as effective heterogeneous nuclei for α-Al. This is due to the 7.4% lattice misfit between the (001) plane of SiC and the (111) plane of α-Al [65]. As a result, the presence of SiC particles increases the number of nucleation agents and refines the grains of α-Al. As shown in Fig. 11(c3), the α-Al grains were found to intermingle at the interface between the SiC_p/A356 layer and the A356 alloy layer. Additionally, the grain sizes of A356 gradually decreased from 196.5 μm to 127.9 μm. The interface of the cladding composite material offers a nearly flawless transition in metallurgy.

3.2. *Microstructure characteristics of powder metallurgy*

In contrast to the methods mentioned earlier, powder metallurgy technology, specifically spark plasma sintering, is a novel and fast solid-state molding technique that allows for precise control of the composition ratio and uniform distribution of the reinforcing phase.

In this study of composites prepared by powder metallurgy, three types of powders were utilized: commercial AlSi10Mg powder with a diameter of 15~53 μm, polyangular micro SiC powder (μm-SiC) with an approximate diameter of 40 μm, and nano SiC powder (nm-SiC) with a diameter of approximately 50 nm. The characteristics of these powders

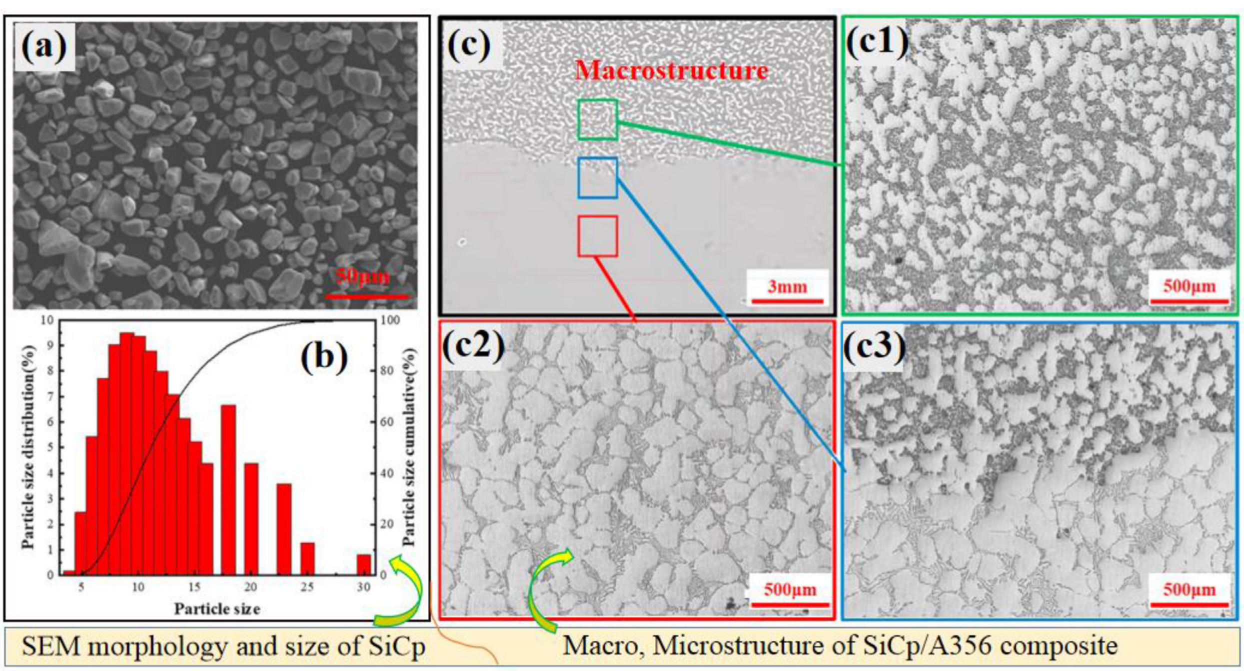

Fig. 11 — (a) Experimental SiC particles SEM morphology and (b) particle size, (c) macrostructures of SiC_p/A356, (c1) microstructures, (c2) A356 layer, and (c3) interface [63].

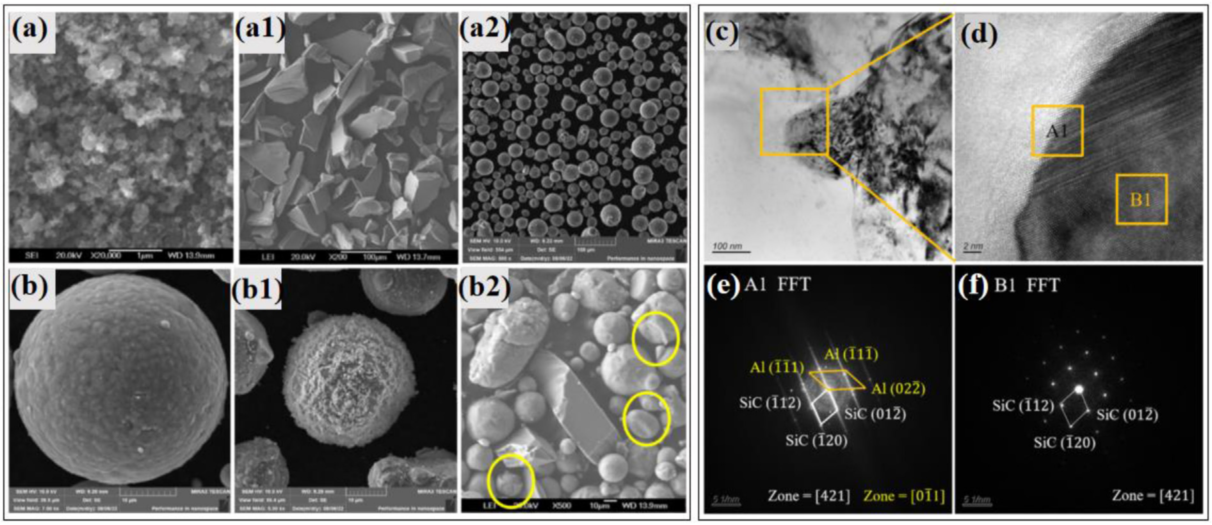

Fig. 12 – SEM images of the raw materials: (a) nm-SiC particles, (a1) mm-SiC particles, (a2) AlSi10Mg powder; (b) AlSi10Mg particle, (b1) mixed powder of 5 wt% nm-SiC particles and AlSi10Mg, (b2) mixed powder of 5 wt% mm-SiC particles and AlSi10Mg; Combinational analysis of TEM and SAED patterns on interface of 5 wt% nm-SiC/AlSi10Mg: (c) AleSiC interface TEM image, (d) higher magnification interface TEM image, (e) SAED pattern of area A1, (f) SAED pattern of area B1 [66].

are illustrated in Fig. 12. The nm-SiC particles, as shown in Fig. 12(a), are mostly circular and flat, and they tend to clump together. The mm-SiC particles, as seen in Fig. 12(a1), are irregular in shape and have sharp edges. The original AlSi10Mg powder, as illustrated in Fig. 12(a2), has a smooth surface and high sphericity.

The process of preparing SiC/AlSi10Mg involves four steps. After four steps of powder mixing, the resulting mixed powder of 5 wt% nm-SiC particles and AlSi10Mg powder showed a uniform adherence of nm-SiC particles to the surface of AlSi10Mg particles, enabling even dispersion in the aluminum matrix. However, the sphericity of AlSi10Mg particles decreased, and the spherical surface was destroyed after ball milling, as shown in Fig. 12(b-b2). And the higher magnification interface TEM images are shown in Fig. 12(c) and (d). These images indicate that the bonding between Al and SiC nanoparticles is strong, and there is no evidence of an Al_4C_3 reaction layer forming at the interface due to the Al–SiC reaction. Additionally, the SAED patterns show that the interface region (A1) contains both SiC and Al matrix phases, while the nanoparticle region (B1) only contains the SiC phase. These findings confirm that the SiC/AlSi10Mg composites produced using the process parameters in this study have a strong interfacial bond and no formation of an interfacial reaction layer.

Jiang et al. [67] studied SiC_p/6061Al composites with different particle sizes and found that the elastic modulus of SiC_p was not significantly affected by the increase in particle size. However, the tensile strength and yield strength gradually decreased, while the shrinkage and elongation of the section initially increased and then decreased. By studying SiC_p/2024Al composites with different volume fractions, Mao et al. [68] found that the tensile strength and hardness of the composites increased with increasing volume fractions. At the same time, certain process factors of powder metallurgy, such as solution and sintering, can also impact the properties of composite materials. For example, Huang et al. [69] studied the effect of solution temperature and time on the microstructure and mechanical properties of 17%SiC_p/Al–Cu–Mg composites. The results showed that the strengthening effect of the solution was not ideal when the solution temperature was low and the solution time was short, resulting in low material strength. However, if the solution temperature is too high, the material is prone to overburning, which reduces its plasticity and strength. The optimal solution temperature and time were 510 °C and 2 h, respectively.

3.3. *Microstructure characteristics of spray deposition*

The surface morphologies of SiC_p and Al feedstock powders were examined using SEM, as shown in Fig. 13. The crushed SiC powders had angular shapes, which are known to result in higher deposition efficiency compared to spherical ceramics. The coarse SiC_p powder had a more uniform particle size compared to the fine powder, as observed at lower magnification. No *trans*-particle cracks were found in either size of SiC particles upon investigation at higher magnification. The aluminum feedstock powder had a uniform size distribution and spherical shape, with only a few larger particles exhibiting satellites when viewed at higher magnification. These defects were not significant enough to affect particle deposition during cold spraying [70], considering the conditions of powder atomization and particle classification.

The microstructure of a four-layer graded Al-SiC_{cp} deposit is shown in Fig. 13(d), which was obtained by increasing the feed rates of SiC_{cp}. The SEM micrograph and EDS mapping, conducted using Sikα radiation (Fig. 13d1), reveal some variations in local distributions. However, the content variation of SiC_{cp} throughout the layer thickness is not clearly defined. This may be due to inhomogeneities within the individual

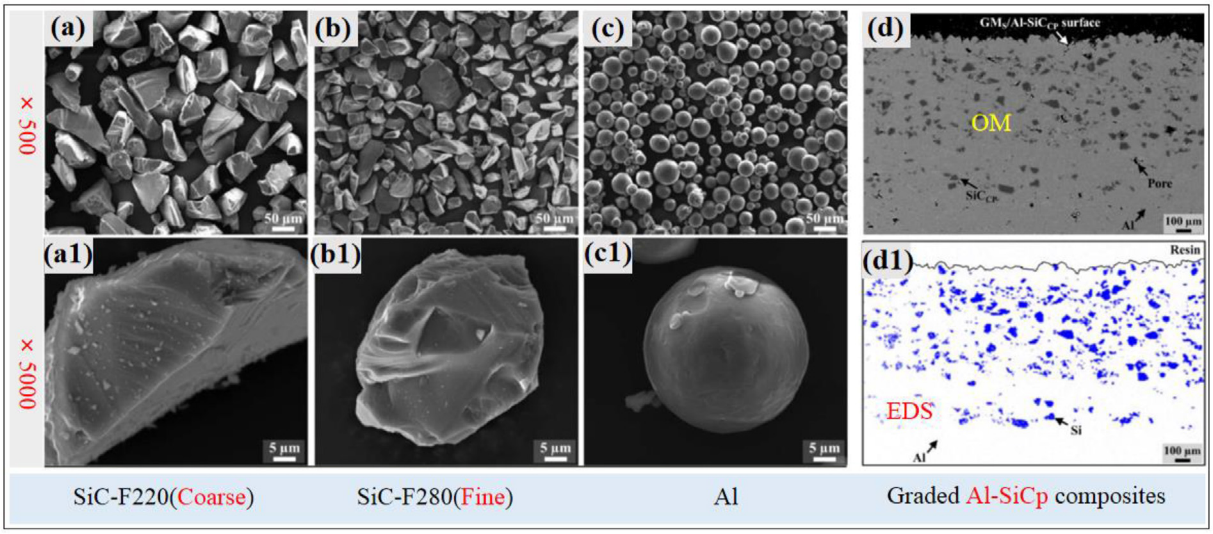

Fig. 13 – SEM micrographs of (a,a1) coarse SiC–F220, (b,b1) fine SiC–F280, and (c,c1) Al; graded Al-SiC$_p$ composites (d) OM and (d1) EDS mapping [53].

layers, similar to those observed in uniformly processed deposits. The alignment of SiC$_p$ depleted zones may overlap with the layer-by-layer adjusted changes in phase compositions. The transition between the individual layers is smooth and barely detectable by optical microscopy (OM), indicating no accumulation of defects at the interfaces between the layers. Therefore, it can be assumed that the compressive strength (CS) of graded composites is not affected by defects and low interlayer cohesion. However, some porosity is observed within the Al matrix, which can be attributed to fragmented SiC$_p$ or pull-out of SiC$_p$ during cross-section preparation, similar to other composite materials. It is worth noting that most of the SiC$_{cp}$ reinforcements are intact.

Aiming at the microstructure and mechanical properties of particle-reinforced aluminum matrix composites, Sun et al. [71] utilized spray co-deposition technology to fabricate rolled composites with a fine and uniform microstructure. There are numerous second-phase particles in the matrix, primarily Al_2CuMg and Al_2Cu phases. As for the high-temperature tensile deformation behavior of particle-reinforced aluminum matrix composites, the tensile flow stress of the composite sheet decreases with the increase in deformation temperature. But the elongation of the composite material is increasing [72,73]. Effective solutions were proposed by [74] to address some metallurgical defects in spray-deposited aluminum matrix composites, such as cracking of SiC particles, pores in the matrix, and interfacial debonding.

3.4. *Microstructure characteristics of ball milling*

To study how reinforcements impact the behavior of ball milling, the shapes of the SiC particle reinforced composite powders were examined using SEM, which is shown in Fig. 14. The microstructure of initial SiC powder and SiC/2024Al composite were shown in Fig. 14(a and b), homogeneity of the structure and distribution of the particles were clearly seen [75].

The interface of the SiC/Al composite and the distribution of elements along the SiC/Al interface are depicted in Fig. 14(d) and e. The line analysis reveals that only a thin layer (10–20 nm) of Mg aggregation can be observed, which has been previously reported [22,73]. Interestingly, a thin oxide layer and an aluminum layer can be observed at the interface between the aluminum matrix and SiC. SiC/Al composites contain numerous small and tough particles, which results in lower resolution compared to other composites. However, this does not hinder the examination of the gain structure of the composites. On the other hand, 2024Al without reinforcements mostly exhibits large, elongated grains with only a few small, equiaxed grains, as shown in Fig. 14(g).

Fig. 14(h) illustrates the impact of ball milling on the microstructure of as-extruded composites. The behavior of composite powders during ball milling is influenced by the type of reinforcement used. In SiC/Al composite powders, some SiC particles are only partially surrounded by the Al matrix, while others are detached from it. Although numerous high-quality SiC$_p$ particles are extracted from the composite powders, they prove to be challenging to be affected by the balls during ball milling. Consequently, only the size of the SiC$_p$ particles that are enveloped within the composite powders is reduced.

3.5. *Microstructure characteristics of spark plasma sintering*

Utilizing lower-cost substrates such as Al and SiC powders through spark plasma sintering, researchers have developed a novel Al–SiC ceramic-matrix composite with a high volume proportion of SiC [76]. The study focuses on analyzing the microstructure and mechanical properties of this composite. The composite was produced by milling 20 wt% Al and 80 wt% SiC powders for 2 h at a speed of 300 rpm, using ethanol and agate balls as the milling medium. The resulting slurry was

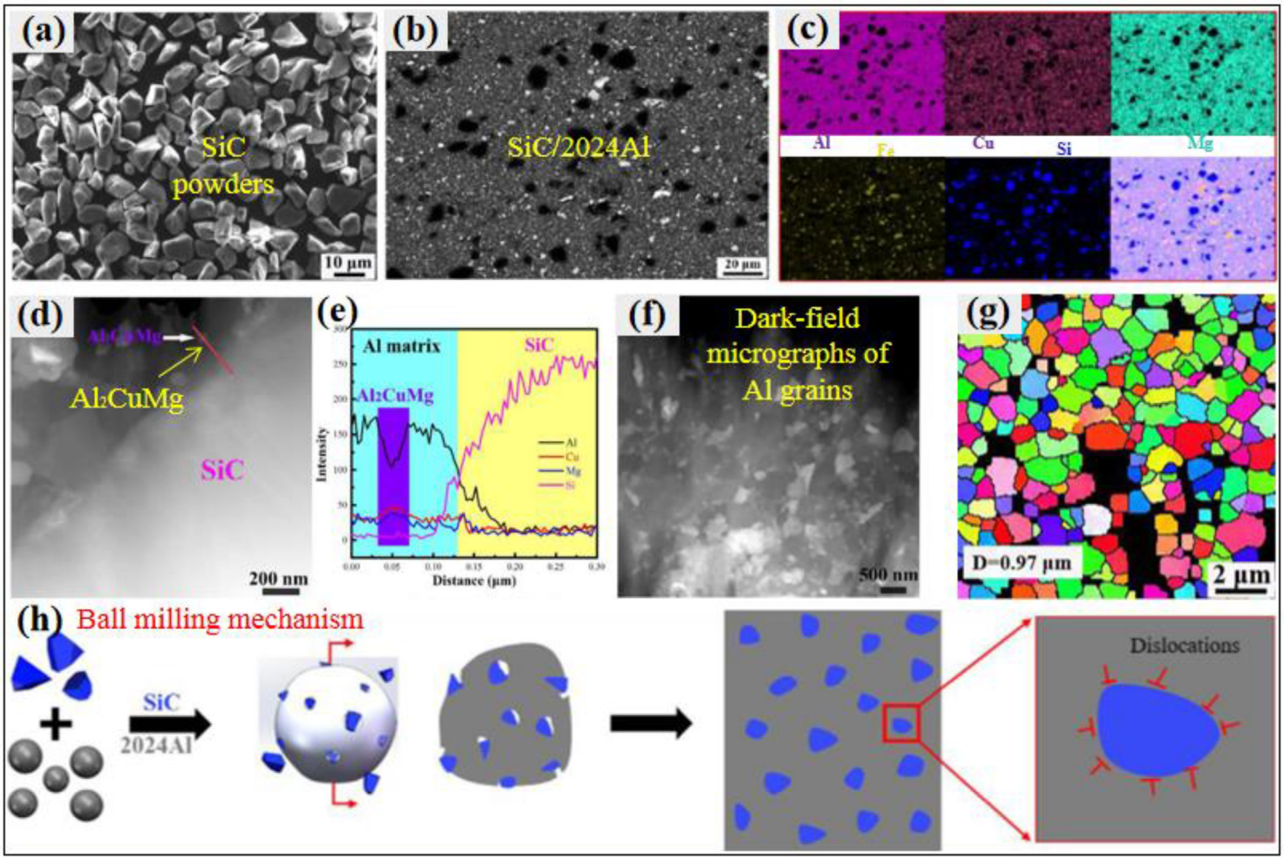

Fig. 14 – Microstructure of (a) SiC powders, (b) SiC/2024Al, (c) EDS elemental mapping, (d,e,f) dark-field image of the interface between 2024Al matrix and SiC_p, (g) IPF image of SiC/2024Al composite, (h) schematic diagram of the ball milling mechanism for SiC/2024Al composite [75].

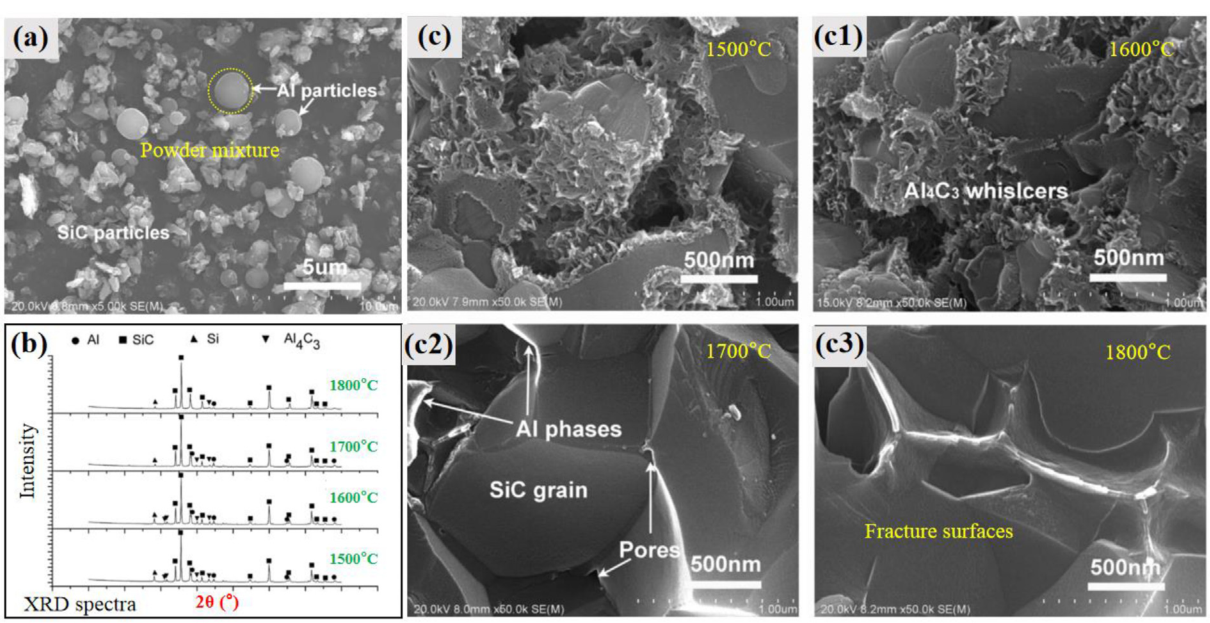

Fig. 15 – Microstructure of (a) powder mixture, (b) XRD spectra of the Al–SiC composites sintered at different temperatures, fracture surfaces of (c-c3) Al–SiC composites sintered at different temperatures: (c) 1500 °C, (c1) 1600 °C, (c2) 1700 °C, and (c3) 1800 °C [76].

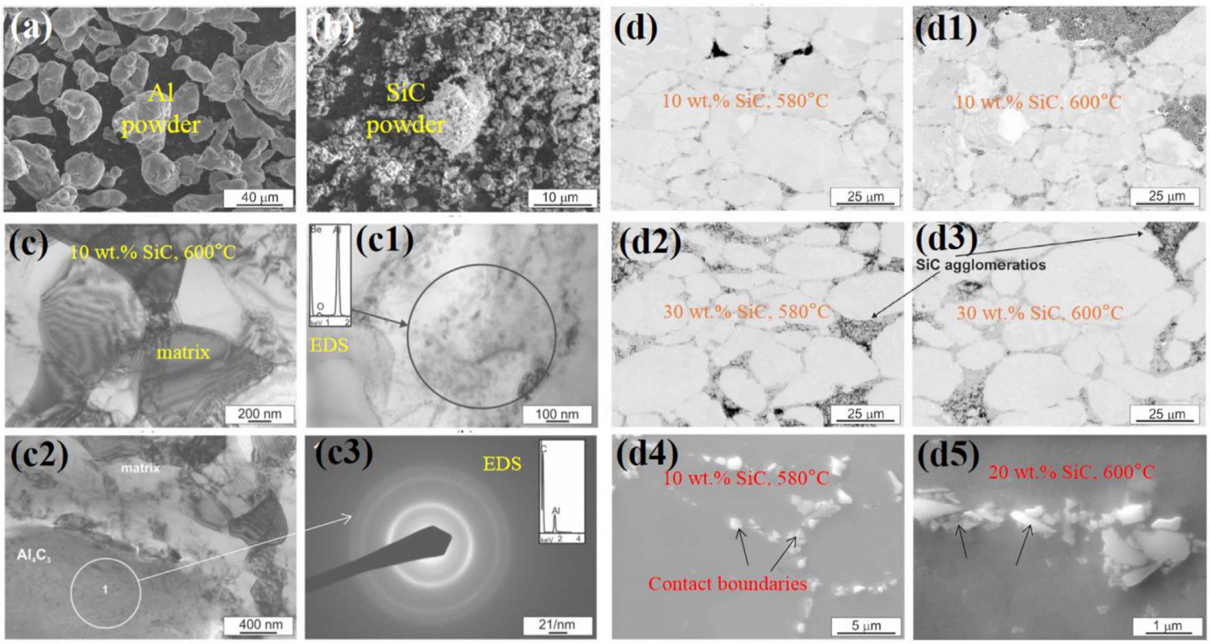

Fig. 16 – Powder particles morphology of (a) Al and (b) SiC; (c-c1) microstructure of spark plasma sintered Al+10 wt% SiC composite in 600 °C, (c2) Al_4C_3 carbide, (c3) diffraction patterns and EDS spectrum from c2; (d) Al+10 wt% SiC in 580 °C, (d1) Al+10 wt% SiC in 600 °C, (d2) Al+30 wt% SiC in 580 °C, (d3) Al+30 wt% SiC in 600 °C, (d4) Al–SiC particle contact boundaries on Al+10 wt% SiC in 580 °C, (d5) Al–SiC particle contact boundaries on Al+20 wt% SiC in 600 °C [77].

vacuum-evaporated to dry it. The spherical aluminum particles are uniformly distributed among the polygonal SiC particles, as indicated by the SEM measurements of the powder mixture shown in Fig. 15(a).

To determine the reaction processes, XRD analysis was initially performed on the reaction products of the sintered samples. The outcomes are displayed in Fig. 15(b). According to the diffraction peaks observed in all of these spectra, the phases present in the specimens are Al, SiC, Si, and Al_4C_3. These phases were obtained through sintering at temperatures ranging from 1500 °C to 1800 °C. However, when the sintering temperature reaches 1700 °C, the intensity of the diffraction peaks for the Al_4C_3 and Si phases noticeably decreases. Furthermore, at a sintering temperature of 1800 °C, the diffraction peak intensities of Al also significantly decrease. This pattern demonstrates a decrease in the volume fraction of the Al_4C_3 and Si phases in the composite sintered at 1700 °C, as well as a similar decrease in the volume fraction of the Al phase in the composite sintered at 1800 °C.

Additionally, as shown in Fig. 15(c) and (c1), a significant number of rod-shaped Al4C3 whiskers were observed scattered on the interface of the SiC grains on the fracture surface of the composites sintered at 1500 °C and 1600 °C. On the fracture surface of the composites sintered at 1700 °C and 1800 °C, only a small number of Al_4C_3 whiskers were observed. The molten aluminum was found on the surfaces of the SiC grains, as shown in Fig. 15(c2) and (c3).The density of the composites increased due to the molten aluminum's ability to fill typical micro-defects such as pores and microcracks during the sintering process.

Al 1070 and SiC had particle sizes of less than 63 µm and 2 µm, respectively, in the original powder. The powders were combined to create the following mixtures: Al, Al+10% SiC, Al+20% SiC, and Al+30% SiC. In a Turbula T2F shaker-mixer, the powder mixtures were prepared. 30 min were spent mixing. Fig. 16(a) depicts the morphology of the Al powder particles, while Fig. 16(b) depicts the morphology of the SiC powder particles. Already in the manufacturing stage, the fine SiC powder has a tendency to form agglomerates (Fig. 16(b)), which are particularly challenging to dissolve during conventional mixing [77].

Observations were done using a TEM to more thoroughly confirm the microstructure of the tested composites. Selected findings are shown in Fig. 16(c)-c3. The subgrains seen near the matrix material (Fig. 16(c), c2) constitute a defining trait of the substructure of the materials under study. The subgrains are less than 1 m in size. Locally, Al_2O_3 clusters and dislocations that create low-energy systems are seen (Fig. 16c1). Al $_2O_3$ particles are no larger than 20 nm in size. An undesirable carbide was found, according to the TEM microstructure analyses that were undertaken (Fig. 16c2). The literature on the casting of Al–SiC composites contains attempts to explain how this compound formed. By examining the impact of the sintering temperature on bending strength, it can be concluded that composites sintered at higher temperatures, such as 600 °C, demonstrate greater bending strengths. It should be observed that the Al sintered compacts produced at both 580 °C and 600 °C did not fracture when bent, demonstrating their high plasticity and strong interparticle bonding. No holes or discontinuities were visible at the grain boundaries were visible in the TEM observations.

There are no discernible variations between the microstructures of the composites that were spark plasma sintered at 580 °C and 600 °C. The reinforcing phase is located between the Al particles in composites sintered at both 580 °C and 600 °C (Fig. 16(d)-d3). Agglomerates are encouraged to develop when the concentration of the strengthening phase of SiC is higher (Fig. 16d2 and d3).Cluster formation is encouraged by the large size differences between the Al particles (< 63 μm) and the SiC particles (< 2 μm). Additionally, the SiC powder had already formed agglomerates prior to the composite production process, as demonstrated by the SEM micrograph in Fig. 16(b). SiC powder particle agglomerates could not be completely eliminated during mixing in the Turbula T2F shaker-mixer. The Al–SiC particle contact border illustrated in Fig. 16d4 andthe SEM micrograph demonstrates a strong bond between these elements. Even in the vicinity of SiC particle clusters, no discontinuities or pores were discovered.

4. Properties characteristics

4.1. *Relative density*

Fig. 17 displays the relative density (RD) of AlSi10Mg and SiC/AlSi10Mg. AlSi10Mg has a high relative density (RD) of 98.83%, indicating nearly complete densification [66]. Even with a 10 wt% increase in μm-SiC, the RD of μm-SiC/AlSi10Mg remains above 98%, with a negligible difference of 0.24% between 2 wt% and 5 wt%. This suggests that the distribution of μm-SiC particles in the matrix is uniform, resulting in a high level of densification. Therefore, the content of μm-SiC has minimal impact on the RD of μm-SiC/AlSi10Mg prepared by SPS. Conversely, the RD of nm-SiC/AlSi10Mg gradually decreases as the nm-SiC content increases, especially when there are high amounts of nano reinforcements present. When the nano reinforcements in SiC/AlSi10Mg composites reach 10 wt%, they tend to agglomerate due to their high specific surface energy. This makes it challenging to sinter and densify the nm-SiC particles during preparation, which leads to an increased number of defects in the final product.

4.2. *Strength*

Compared to pure Al, the engineering stress of SiC_{np}/AMCs and $SiC_{\mu p}$/AMCs has been improved, and the tensile strength of SiC_{np}/AMCs has increased to 435 MPa, which is 292% higher than that of pure Al. This is illustrated in Fig. 18(a and b). The strength of AMCs increases to 200 MPa, which is only 135% of that of pure Al. According to the Hal-Petch relationship [78], the smaller the grain size, the higher the grain boundary density, and the more difficult it becomes to impede dislocation movement, thus increasing resistance to plastic deformation.

In order to achieve a balance between strength and ductility through the optimization of SiC particles, a diagram was presented in Fig. 18(c). SiC_{np}/AMCs have uniform, ultrafine grains with intragranularly dispersed SiC particles that promote the dynamic recrystallization (DRX) process and increase stability through the Zener pinning mechanism. $SiC_{\mu p}$/AMCs had a multimodal grain microstructure with micro-sized and ultra-fine grains, which were enhanced by fractured micro-SiC particles during the DDM process. SiC_{np}/AMCs exhibit high strength due to grain boundary and Orowan strengthening mechanisms, whereas $SiC_{\mu p}$/AMCs demonstrate enhanced ductility as coarse grains can accommodate stress-relaxation from ultra-fine grains. By optimizing SiC particles, the specific microstructure of SiC/AMCs can be designed to achieve a balance between strength and ductility. Nano-SiC particles enhance the strength of the matrix, while micro-SiC particles contribute to excellent ductility.

Fig. 18(d and e) illustrates the impact of sintering temperature on the bending strength of composites made with different SiC particle sizes and Al alloy compositions. Effective

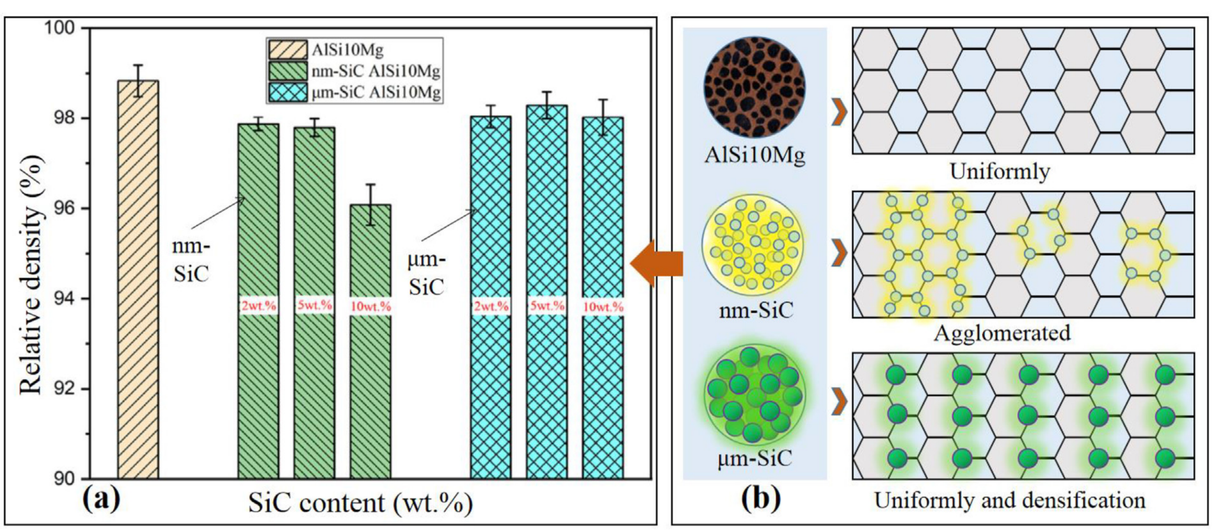

Fig. 17 – (a) Relative density of AlSi10Mg and SiC/AlSi10Mg with different SiC contents, (b) schematic diagram of particle agglomeration [66].

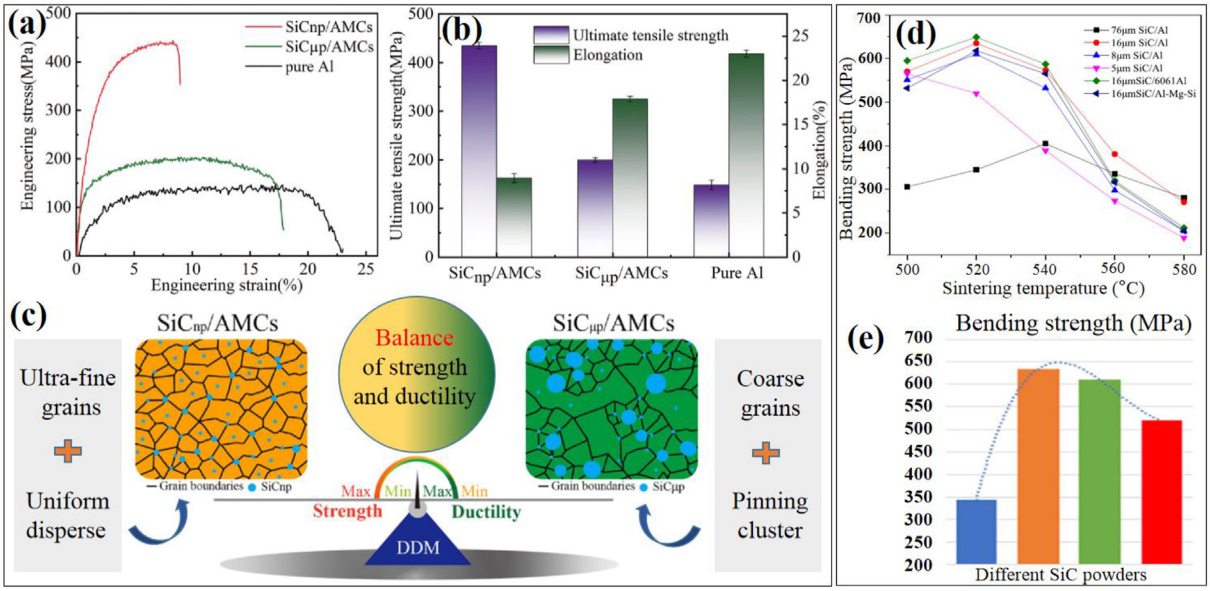

Fig. 18 – Mechanical performances of deformation-driven metallurgy samples: (a) typical engineering stress-strain curves and (b) ultimate tensile strength/elongation of SiCnp/AMCs, $SiC_{\mu p}$/AMCs, and pure Al, (c) strategy in the strength-ductility balance via optimizing SiC particles, (d) bending strength in different sintering temperature, (e) bending strength of the SiC/Al composites with different SiC powders [52].

interface bonding promotes heat conduction during thermal conductivity. However, the presence of numerous pores within the material can hinder this process by scattering phonon thermal motion and trapping gas with low thermal conductivity. When the SiC volume fraction was kept constant, the interfacial bonding deteriorated, and the coefficient of thermal expansion increased as the material density decreased. The best physical properties were observed in the 16 μm SiC/Al composite made with 6061Al alloy as the matrix material, sintered at 50 MPa, 8 min, and 520 °C. This composite exhibited a high bending strength of 649 MPa, as depicted in Fig. 18(e)).

4.3. *Hardness*

Brinell hardness testing was performed according to ASTM E10. Samples with dimensions of 20mm × 12 mm were prepared according to ASTM standards, as shown in Fig. 19(a and b). The stiffness test uses a load of approximately 187.5 kgf for a duration of 30 s. Hardness is calculated based on the recorded depth of indentation. Three indentation tests were performed on each sample, and the average of the three tests was used to predict the hardness [80].

The diagram in Fig. 19(d) illustrates the changes in hardness of MMCs when SiC is added in different weight percentages, both with and without heat treatment. The findings indicate that as the amount of SiC particles increases, the hardness of MMCs also increases by 22.58%. This increase in hardness is attributed to the presence of hard ceramic particles, such as SiC, in the soft aluminum alloy A356 matrix. However, the hardness of the heat-treated sample decreases by up to 6.5% due to the relaxation of internal stresses.

Fig. 19(e) displays the hardness of a pure material with a Rockwell hardness value of 90 RHB [81]. However, in the composite specimens, the hardness value ranged from 102 to 114, increasing with the duration and speed of stirring. The highest hardness value was achieved at a 27% increase compared to the pure material, and it was obtained when the process parameters were set to their upper limits. When the stirring speed and time were increased, it was observed that the distribution of SiC particles in the aluminum metal matrix became more uniform. This led to an increase in the hardness of the Al8011–SiC composites.

Wu [82] and Jiang [83] prepared SiC_p/Al composites with different volume fractions using the liquid-phase method and semi-solid method, respectively. The study found that, under conditions of good interfacial bonding, the wear resistance and hardness of the composites increased with the increase in the volume fraction of SiC particles. Additionally, the tensile strength initially increased and then decreased, while the elongation gradually decreased. Li et al. [84] found that injecting Al-SiC_p composite powder into semi-solid alloy liquid promotes interfacial wettability and uniform distribution of reinforced particles. This process also increases hardness and reduces porosity.

4.4. *Elasticity modulus*

The elastic modulus is the most significant mechanical property of composites reinforced with particles. The factors that affect the elastic modulus of particle-reinforced aluminum matrix composites include the shape, volume fraction, and distribution of the particle-reinforced phase. Generally, the elastic modulus increases with an increase in

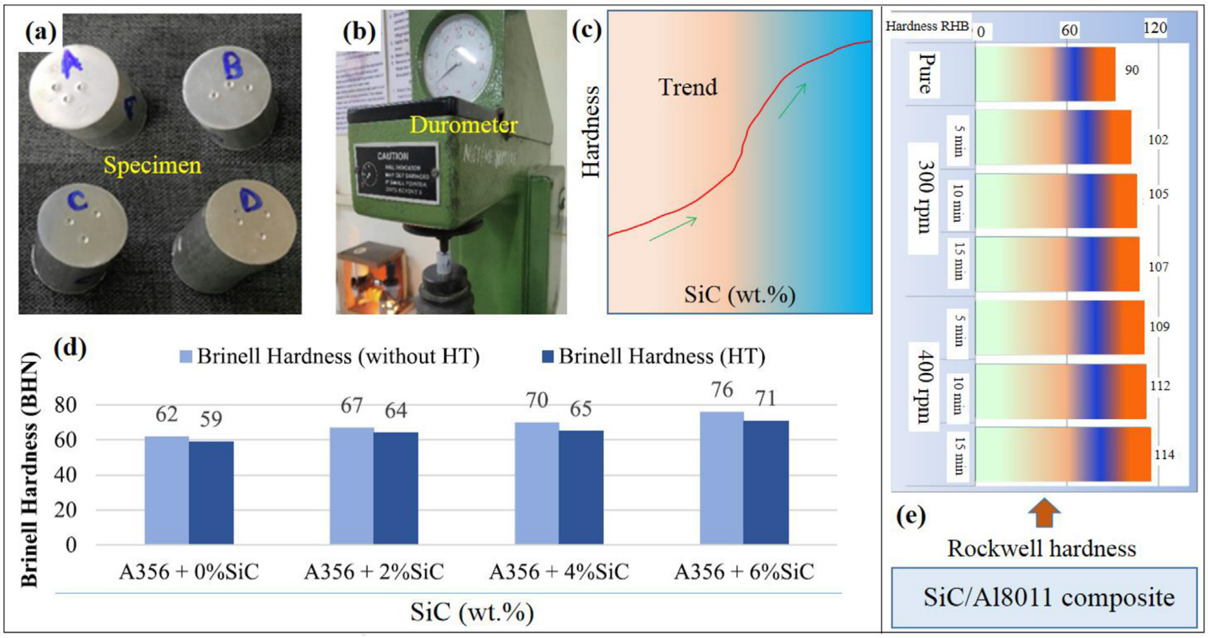

Fig. 19 – (a) Heat-treated specimen for hardness test, (b) brinell hardness of the specimen, (c) variation trend of hardness with SiC content, (d) effect of SiC on hardness with and without heat-treatment MMCs [80], (e) rockwell hardness of different specimens [81].

the volume fraction of the reinforced particles. However, the impact of the shape of the reinforced phase on the elastic modulus is not well understood.

Regarding the elastic modulus of particle-reinforced metal matrix composites, the simple mixing method has a relatively large calculation error. Additionally, the calculation formula for the series structure does not account for the inconsistency in side shrinkage between the reinforced phase and the matrix two-phase materials. In recent years, the Halpin-Tsai formula has been widely used in research work [85].

$$E = E_m\left(1 + 2sqV_p\right) \Big/ \left(1 - qV_p\right) \quad (1)$$

$$q = (E_p - E_m) / (E_p + 2sE_m) \quad (2)$$

In the formula, E, E_m and E_p represent the elastic modulus values of composite material, matrix and reinforced particles respectively, while s and V_p represent the length-diameter ratio and volume fraction of reinforced particles respectively. When the particle shape is regular and the distribution is uniform, the s value will be better determined and the calculated value will be more accurate.

The elastic modulus of the aluminum alloy matrix is approximately 70 GPa, whereas the elastic modulus of SiC particles is around 450 GPa. According to theoretical analysis, the higher the volume fraction of SiC particles, the higher the elastic modulus of the composites will be. The results show that when the volume fraction of SiC particles is less than 30%, the elastic modulus of the composites increases linearly with the addition of SiC particles. However, when the volume fraction of SiC particles is too high, the mechanical properties of the composites are reduced due to particle agglomeration and the challenge of effectively dispersing the reinforced particles.

4.5. *Fracture toughness*

Fracture toughness characterizes a material's ability to resist fracture deformation. Fracture toughness, K1c, generally decreases with decreasing particle size or increasing volume fraction of reinforced particles. The nucleation of cracks in particle-reinforced aluminum matrix composites generally occurs in the region where particles are segregated. The critical stress for nucleation is not determined by the overall volume fraction of reinforced particles, but rather by the volume fraction of locally reinforced particles. Most scholars believe that the fracture is caused by the separation of particles or the detachment between the matrix and particles. Large particles in the matrix of high strength tend to fracture, while pores in the matrix of low strength preferentially nucleate at the interface.

Hosseinzadeh et al. [86] studied SiC/Al2024 composites after hot extrusion and found that the fracture toughness of the composites was closely related to the length-to-diameter ratio and volume fraction of SiC particles. When the volume fraction of SiC particles increases from 3% to 10%, the fracture toughness of the material decreases from 20.16 MPa $m^{1/2}$ to 14.67 MPa $m^{1/2}$, as shown in Fig. 20. Song et al. [87] tested SiC particle reinforced Al–Cu–Mg composites and found that the fracture toughness of the composites decreases as the volume fraction of SiC particles increases. They also observed that the evolution of fracture toughness is opposite to that of yield stress during aging. Furthermore, increasing the aging

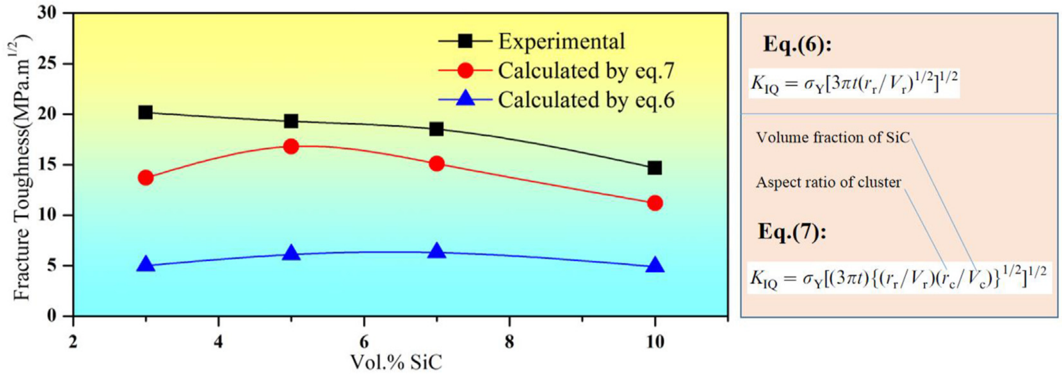

Fig. 20 – Comparison of the experimental and calculated (according to Eqs. (6) and (7)) fracture toughness values as a function of the volume percentage of SiC in the composites [86].

temperature can enhance the minimum fracture toughness of the composites.

4.6. Wear behavior

In composite materials, the wear behavior is influenced by various factors including the geometry, orientation, composition, size, type of reinforcement, heat treatment regimen, load, and sliding speed [88,89]. According to a comprehensive investigation of the wear mechanism, the main types of wear in metal matrix composites are abrasive wear and adhesive wear. The primary form of wear is delamination, which occurs due to the development and spread of subsurface fissures [90].

In terms of particle content, the wear volume of SiC_p/ZL102 composite decreases with the increase of SiC_p content and reaches its minimum at approximately 25 vol%. When the volume fraction exceeds 33 vol%, it increases. Due to the increase in the number of particles, the proportion of hard points increases, which strengthens the matrix and improves wear resistance. However, if the content is too high, the particles are prone to aggregation, resulting in defects [91,92]. Ravi Kumar et al. [93] studied the dry sliding wear resistance of SiC_p and Al_2O_3 reinforced Al composites and found that the wear of the material decreased significantly when the particle content increased from 5 vol% to 20 vol%. However, under abrasive wear conditions, when the content of Al_2O_3 or SiC_p increases from 5% to 20%, there is a slight increase in wear when the load is less than 45 N. However, wear decreases significantly at 89 N and 134 N. When the NbC_p content increases from 0% to 60%, the wear rate of NbC_p/Ni–Cr composites consistently decreases.

The wear resistance of the material is also affected by particle size. The investigation on the wear resistance of 20 wt % Al_2O_3/Al composite revealed that the material with a particle size of 142 μm exhibits greater wear resistance compared to the smaller particle materials (16 μm and 63 μm). This is because the matrix wears more quickly, causing the larger particles to remain on the contact surface for a longer period of time in abrasive wear. The foundation, of course, is strong interface bonding. However, the experimental results on sliding friction and wear under lubricating conditions demonstrate that the wear rate of the SiC_p/2124Al composite increases with an increase in particle size [94].

4.7. Damage behavior

The static tensile damage behavior of particle-reinforced metal matrix composites depends on several factors [95,96]. These factors include the volume percentage of the particles, the type, shape, and size of the particles, and the microstructure of the matrix. These factors directly influence the strength of the particles and the strength of the particle/matrix interface. The combination of these two strength factors determines the damage and fracture characteristics of the material.

Two basic modes of damage evolution and fracture are shown in Fig. 21. If the strength of the particles is lower than the strength of the particle/matrix interface, multiple particles crack before the interface during the tensile process, leading to the formation and growth of micro-pores in the matrix [97]. At the same time, local shear occurs among the cracked particles, which eventually leads to material failure (upper side of Fig. 21). If the strength of the particles is greater than the strength of the interface, multiple interfaces will crack first during the tensile process. These cracks will then expand in the matrix and connect with each other, ultimately resulting in material failure (as shown in the lower side of Fig. 21). Therefore, due to the low-power morphology of the fracture surface, the fracture often does not exhibit distinct partition characteristics, such as a fiber zone, radiation zone, or shear lip zone.

For a SiC particle-reinforced aluminum matrix composite, the process of tensile fatigue crack propagation was studied using in-situ synchrotron radiation X-ray three-dimensional tomography. It was found that the material damage was mainly caused by the crack bypassing the reinforced particles at a low stress ratio (e.g. 0.1), in which only a few particles cracked. Under the condition of a higher stress ratio (e.g., 0.65), the SiC particles in front of the crack tip fracture, and subsequently, the crack propagates forward through the particles, as depicted in Fig. 21(b)–(d), where red represents the crack, green represents SiC particles, and blue represents cracked

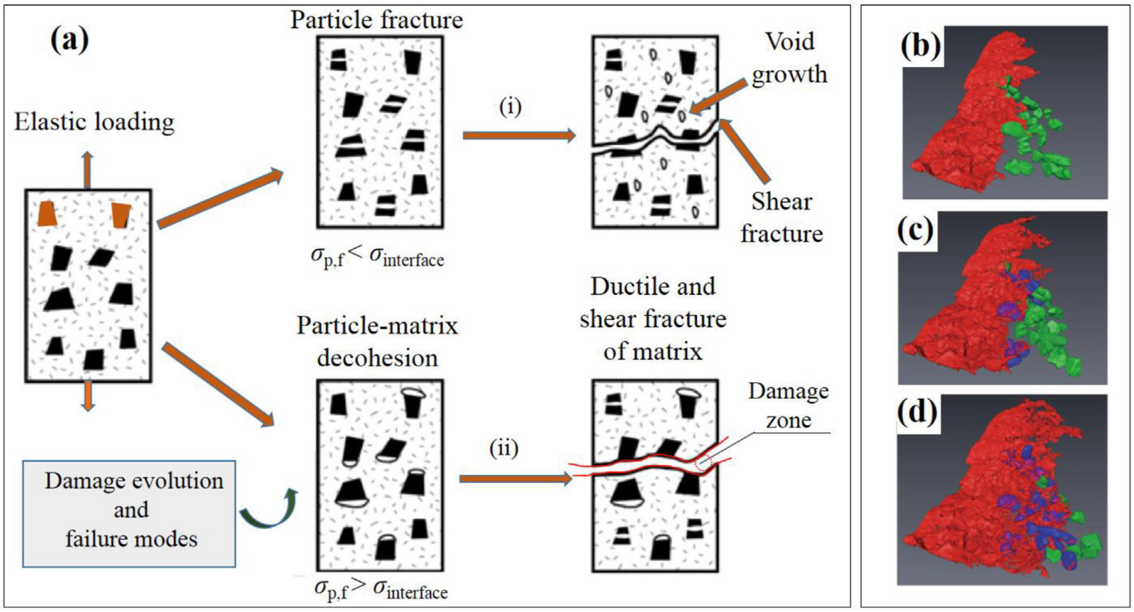

Fig. 21 – (a) Two fundamental modes of damage evolution and failure of particle reinforced metal matrix composites under static tension loading, (b–d) fatigue crack propagation mechanism of a SiC particle reinforced Al composite under the stress ratio of 0.65 at 0 cycle, 6000 cycles and 17,000 cycles respectively [97].

SiC particles. Similarly, under low stress intensity factor (SIF) or maximum SIF conditions, fatigue crack propagation primarily bypasses the particles. However, under high SIF or maximum SIF conditions, the particles in front of the crack tip fracture, resulting in a relatively flat crack propagation path.

5. Influence factors of properties

5.1. *Particles*

The beneficial combination of SiC particle reinforcement and matrix metal results in the new composites being stable in size, having a small thermal expansion coefficient, high temperature resistance, fatigue resistance, fracture resistance, aging resistance, and corrosion resistance. Therefore, SiC particle reinforcement is highly likely to be applied in actual production. Regarding particle-reinforced aluminum matrix composites, the quantity of added particles has a significant impact on the microstructure, hardness, porosity, and other properties of the composites. This, in turn, determines the mechanical and wear-resistant properties of the prepared composites. In SiC_p/A356 aluminum matrix composites prepared using the semi-solid stirring method, the distribution uniformity of SiC particles in the matrix gradually increases with the higher amount of SiC particles. When the volume fraction of SiC particles is 25%, the distribution of SiC particles in the aluminum alloy matrix is the most uniform. With the increase in SiC particles, the porosity and hardness of SiC_p/A356 aluminum matrix composites gradually increase [13,63]. The higher the volume fraction of SiC particles in SiC_p/A356 aluminum matrix composites, the more uniform the particle distribution, and the higher the wear resistance.

5.2. *Strengthening mechanism*

The strengthening effect of the composites mainly depends on the type and content of the reinforcement, as well as the type of alloy matrix and the heat treatment state of the composites. It is generally believed that there are two mechanisms for strengthening metal matrix composites: direct strengthening and indirect strengthening.

Therefore, direct strengthening primarily involves the transfer of load from the matrix to the reinforcement phase. It also includes the reinforcement body's effect on constraining the deformation of the matrix or obstructing the movement of dislocations within the matrix. Additionally, it encompasses the generation of thermal residual stress in the matrix and the work hardening of the matrix. Indirect strengthening refers to the influence of the reinforcement phase on the microstructure or deformation mode of the matrix. This includes the bonding state of the interface between the matrix and the reinforcement, as well as the enhancement of the microstructure of the matrix near the interface in the composite material. The strengthening mechanism provides theoretical support for the preparation of high-performance Al matrix composites [14,28]. The research on the strengthening mechanism of SiC_p/Al composites by heat treatment mainly focuses on indirect strengthening. This refers to the influence of interface bonding and secondary precipitation on the relative strength of SiC_p/Al composites [30,76].

In addition, the dispersion of reinforced particles with high hardness and high elastic modulus in the aluminum matrix will inevitably impede the movement of dislocations. When the spacing between reinforced particles is sufficiently large, the hardness becomes high enough to resist the cutting effect of dislocations. As a result, the motion of dislocations is impeded, and they can only protrude from the reinforcing particles. Eventually, these dislocations join together and continue to move, leaving a dislocation ring around the reinforcing particles. This ring blocks the movement of dislocation lines passing through it, thereby strengthening the composite matrix. Generally, as the reinforcement particle content increases, the spacing between particles effectively decreases. This enhances the ability to impede the movement of dislocations in the matrix, resulting in a more pronounced Orowan strengthening effect.

5.3. *Interfacial reactions*

At temperatures of 700 °C–900 °C, the SiC particles did not exhibit good wettability with the molten Al alloy. However, as the temperature increased, the interfacial wettability improved. At high temperatures, there is a risk of forming a brittle and hydrolysable Al_4C_3 phase [98]. If the sintering temperature of the composite exceeds the melting point range of the Al alloy, the Al alloy will transform into a molten state during sintering. When SiC particles come into contact with the Al alloy liquid, they would begin to dissolve. As the carbon concentration reached saturation at the interface, Al_4C_3 would grow into the Al alloy liquid in block and needle shapes within the Al alloy liquid.

SiC particles react with liquid aluminum at the interface, resulting in the formation of a low-density product called Al_4C_3, which predominantly coats the SiC particles. This greatly reduces the density difference between the reinforced particles and the aluminum alloy melt. Interfacial reaction is closely related to temperature and reactant concentration, but since the latter remains unchanged in this system. Therefore, controlling the temperature can regulate the interfacial reaction [99–101].

$$4Al + 3SiC \rightarrow Al_4C_3 + 3Si \tag{3}$$

Due to the unique nature of the extrusion casting method, it cannot provide favorable thermodynamic and kinetic conditions for the reactions described in formula (3). The use of squeeze casting to facilitate pressure infiltration of SiC particle preforms with high-purity Al effectively prevents the formation of Al_4C_3. The contact time between the reinforced particles and the molten aluminum was reduced due to the cooling effect of the preform and the mold, resulting in a decrease in the likelihood of interfacial reactions. Another process involves preheating the SiC material to 600 °C, which promotes the formation of SiO_2 oxidation layers on the SiC particles [102]. Al_4C_3 cannot form due to the presence of SiO_2 layers, which prevent direct contact between the molten Al and the SiC.

6. Application

6.1. *In automobiles*

Particle-reinforced AMC is particularly suitable for manufacturing anti-wear materials [103], such as piston rings and bearing bushes. Toyota Motor Company has utilized SiC particle-reinforced AMC material for producing piston rings and engine connecting rods. In addition, the SiC particle-reinforced AMC material can also be used to manufacture cylinder linings, drive shafts, and other automotive parts [104].

6.2. *In aerospace*

In the aerospace industry, SiC particle-reinforced AMCs are used to manufacture load-bearing compression rods, guide rails, and taxiing landing devices for helicopters, missile inlay structures, and universal antenna stands, among other applications. In addition, the use of particle-reinforced AMCs in satellites has been reported [105].

6.3. *In precision instrument*

SiC particle-reinforced AMCs have higher micro yield strength and compression resistance, making them potential replacements for beryllium alloy in inertial navigation devices [106]. In the infrared homing and guiding system, replacing the original stainless steel with SiC particle reinforced AMCs to manufacture universal joint parts can reduce the weight by 62%. In addition, SiC particle-reinforced AMCs can also be used to manufacture laser gyroscopes.

6.4. *Optical instrument*

The United States has developed an ultra-light space telescope that utilizes SiC particle-reinforced AMC material for its bracket, support, and secondary mirror. This innovation significantly reduces the overall mass of the telescope. By controlling the content of SiC particles, the thermal expansion of the composite can be matched with that of the reflection layer, thereby achieving ideal stability over a wide temperature range [107]. In addition, SiC particle-reinforced AMCs can also be used to replace beryllium and other precious metal materials in the infrared observation mirror and launch control mirror of tactical tanks [108].

7. Conclusion and outlook

After nearly 30 years of research and development, particle-reinforced AMCs are now rapidly moving towards commercial production and application [71,109,110]. The key factors that have been limiting the development of particle-reinforced AMCs, such as complex processes and high costs, are gradually being eliminated. The United States, Europe, Japan, and other countries have invested significant financial and material resources in establishing factories for industrial-scale production of particle-reinforced AMCs. These factories produce dozens of product types and specifications that have been applied in various fields such as aerospace, military, electronics, automobiles, and sports equipment. The particle-reinforced AMCs have entered a stage of rapid growth. In the 21st century, China's economy and military will further develop, and many fields (such as aerospace, military, electronics, and automobile industries) will undoubtedly demand higher-quality materials for their development. These requirements present opportunities for the advancement of particle technology. Nevertheless, this requirement provides opportunities for the development of particle-reinforced AMCs.

There are many types of particle-reinforced AMCs [85,113–115], each of which has different composite effects, interface structures, design methods, and preparation processes. The testing of performance stability during service is also a major challenge. Therefore, most high-performance particle-reinforced AMCs have long research and development cycles and a high risk of failure. Only governments can afford to invest significant amounts of money in this challenging task. Particle-reinforced AMCs are a key area of research and development in MMCs, owing to their exceptional performance [26,27,116]. The potential for development in this area is extensive, and it is highly likely that these materials will be widely produced and utilized. This widespread production and application are expected to catalyze a significant transformation in the field of advanced material applications [71,91,117].

Some conclusions of this review paper are summarized as following.

(1) SiC particle-reinforced MMCs have broad application prospects in the aerospace industry, automobile industry, internal combustion engine industry, military industry, and electronic civil industry. This is due to their high specific stiffness, low coefficient of thermal expansion, good wear resistance, heat resistance, and excellent high-temperature strength.
(2) The equipment used in stir casting is simple and easy to operate. However, it is difficult to achieve even mixing of the single reinforcement with the matrix material, and there is a significant issue of material absorption. Composites prepared by powder metallurgy have significantly increased strength and hardness at both room temperature and high temperature. They also exhibit improved wear resistance and can be tailored to achieve various types of composites, allowing for the full utilization of each component material's characteristics. Powder metallurgy is a cost-effective process technology for producing high-performance composite materials. Extrusion casting can significantly enhance the strength, Young's modulus, and plasticity of composite materials. The process and equipment involved are simple, and the resulting structure is dense, free from porosity, and exhibits stable material quality. As a result, extrusion casting has found widespread application in industrial production. The process cycle time of the spray deposition method is short, and the forming speed is fast. However, there are disadvantages such as expensive equipment, porosity, and raw material loss.
(3) The use of relatively traditional methods for preparing SiC particle-reinforced aluminum matrix composites is gradually decreasing. The new techniques, such as the high-energy ultrasonic semisolid composite method and high-energy ball milling method, have generated significant interest among scholars, leading to extensive research being conducted. These new techniques for preparing SiC_p/Al composites have outstanding performance advantages and promising application prospects in the automotive and aerospace fields. They have significantly contributed to the development of the automotive and aerospace industries.

Finally, the SiC particle-reinforced AMC has excellent performance [118–123] and low cost. Combined with the domestic and foreign particle-reinforced AMCs and the current application scenario, future research on SiC particle-reinforced AMCs can focus on the following aspects.

(1) It is possible to enhance the preparation process and research level of particle-reinforced AMCs. The effectiveness and cost of composite materials are directly influenced by the level of preparation [124,125]. Hence, it is imperative to develop innovative methods for composite preparation, optimize process parameters, and strengthen equipment construction. Such measures are crucial for enhancing the techniques of the preparation process, and research in this field holds immense significance.
(2) An alternative approach to enhancing the technological advancement of particle-reinforced AMCs involves optimizing the subsequent heat treatment process [126–128]. A critical aspect of particle-reinforced composites pertains to the interfacial bonding between the reinforcement and the matrix alloy. Enhancement of the subsequent heat treatment method can improve the interfacial bonding, allowing for the adjustment of the composite's performance to the desired optimal state.
(3) Machining proficiency of particle-reinforced AMCs, including SiC particle-reinforced AMCs, can be enhanced through appropriate cutting techniques, selection of processing technology, and development of tool materials [129]. The high hardness of the reinforcement particles in particle-reinforced AMCs results in increased tool wear during mechanical processing. Therefore, implementing suitable cutting methods, selecting appropriate processing technology, and developing suitable tool materials can effectively reduce costs and conserve materials.
(4) There is actually an approach that can be taken to improve the connection technology of particle-reinforced AMCs at the level. AMCs are non-homogeneous, multi-phase materials, and their connection is much more complicated than that of single-phase homogeneous materials [130–132]. An effective and economical joining technology for SiC particle-reinforced AMCs needs to be developed for industrial applications. The effective and economical joining technology is one of the urgent issues in the industrial application of SiC particle-reinforced AMCs.
(5) The reinforcement of particle-reinforced AMCs forms galvanic coupling corrosion with the matrix alloy, which accelerates the corrosion rate, even though it improves the corrosion resistance of particle-reinforced AMCs. Enhancing the corrosion resistance of particle-reinforced AMCs is a crucial area of research in order to make them suitable for various environments [133,134]. The advancement and refinement of the

manufacturing process will facilitate the widespread utilization of SiC particle-reinforced AMCs in various industries.

Data availability

All data generated or analyzed during this study are included in this published article.

Declaration of competing interest

The authors declare that they have no known competing financial interests or personal relationships that could have appeared to influence the work reported in this paper.

Acknowledgments

This work was supported by the Science and Technology Research Program of Chongqing Municipal Education Commission KJQN202001301 and the Industry-University-Research Cooperation Program (WLHX-2020-0048, WLHX-2022-0162).

REFERENCES

[1] Melaibari A, Fathy A, Mansouri M, Eltaher MA. Experimental and numerical investigation on strengthening mechanisms of nanostructured Al-SiC composites. J Alloys Compd 2019;774:1123–32. https://doi.org/10.1016/j.jallcom.2018.10.007.

[2] Fathy A, Wagih A, Abu-Oqail A. Effect of ZrO_2 content on properties of Cu-ZrO_2 nanocomposites synthesized by optimized high energy ball milling. Ceram Int 2019;45:2319–29. https://doi.org/10.1016/j.ceramint.2018.10.147.

[3] Khdaira AI, Fathy A. Enhanced strength and ductility of Al-SiC nanocomposites synthesized by accumulative roll bonding. J Mater Res Technol 2020;9:478–89. https://doi.org/10.1016/j.jmrt.2019.10.077.

[4] Liu L, Li SF, Zhang X, Pan D, Gao LN, Chen B, et al. Syntheses, microstructure evolution and performance of strength-ductility matched aluminum matrix composites reinforced by nano SiC-cladded CNTs. Mater Sci Eng A 2021;824:141784. https://doi.org/10.1016/j.msea.2021.141784.

[5] Song MX, Peng K. Pre-oxidization of SiC on interfacial structure and mechanical properties of SiC_p/Al composites prepared by vacuum-pressure infiltration. J Mater Res Technol 2023;24:6567–77. https://doi.org/10.1016/j.jmrt.2023.04.246.

[6] Murugandhan D, Valli R, Senthilkumar N, Arunmozhi S. Enhancement of energy storage capacity in lithium polymer batteries incorporated with zirconium oxide nano powders. Mater Today Proc 2020;37:1313–9. https://doi.org/10.1016/j.matpr.2020.06.468.

[7] Ahmad I, Islam M, Subhani T, Zhu Y. Toughness enhancement in graphene nanoplatelet/SiC reinforced Al_2O_3 ceramic hybrid nanocomposites. Nanotechnology 2016;27:425704. https://doi.org/10.1088/0957-4484/27/42/425704.

[8] Ahamad N, Mohammad A, Gupta P. Wear characteristics of Al matrix reinforced with Al_2O_3-carbon hybrid metal matrix composites. Mater Today Proc 2021;1:63–8. https://doi.org/10.1016/j.matpr.2020.05.739.

[9] Jayakumar K. Machining of TiB_2-SiC ceramic composites through WEDM process. Mater Sci Forum 2020;979:22–7. https://doi.org/10.1016/j.jmapro.2022.02.013.

[10] Vijayabhaskar S, Rajmohan T. Experimental investigation and optimization of machining parameters in WEDM of nano-SiC particles reinforced magnesium matrix composites. Silicon 2019;11:1701–16. https://doi.org/10.1007/s12633-017-9676-0.

[11] Velavan K, Palanikumar K. Analysis on sliding wear behavior of Al+B_4C+mica hybrid metal matrix composites. Mater Express 2020;10:986–97. https://doi.org/10.1016/j.jmrt.2020.12.004.

[12] Abdallah R, Soo SL, Hood R. The influence of cut direction and process parameters in wire electrical discharge machining of carbon fibre–reinforced plastic composites. Int J Adv Manuf Technol 2021;113:1699–716. https://doi.org/10.1016/j.procir.2018.08.284.

[13] Lee H, Sohn SS, Jeon C, Jo I, Lee SK, Lee S. Dynamic compressive deformation behavior of SiC-particulate-reinforced A356 Al alloy matrix composites fabricated by liquid pressing process. Mater Sci Eng A 2017;680:368–77. https://doi.org/10.1016/j.msea.2016.10.102.

[14] Zhang J, Shi H, Cai M, Liu L, Zhai P. The dynamic properties of SiC_p/Al composites fabricated by spark plasma sintering with powders prepared by mechanical alloying process. Mater Sci Eng A 2009;527:218–24. https://doi.org/10.1016/j.msea.2009.08.067.

[15] Ahmed A, Neely AJ, Shankar K, Nolan P, Moricca S, Eddowes T. Synthesis, tensile testing, and microstructural characterization of nanometric SiC particulate-reinforced Al 7075 matrix composites. Metall Mater Trans A 2010;41:1582–91. https://doi.org/10.1007/s11661-010-0201-y.

[16] Narale MN, Kulkarni SG, Menghani JV, Lal A. Experimental investigation and optimization of multiple performance characteristics of Al-Mica-B_4C hybrid reinforced composite in drilling operation. Mater Today Proc 2018;5:19763–72. https://doi.org/10.1016/j.matpr.2018.06.339.

[17] Carvalho O, Buciumeanu M, Madeira S, Soares D, Silva FS, Miranda G. Dry sliding wear behaviour of AlSi-CNTs-SiC_p hybrid composites. Tribol Int 2015;90:148–56. https://doi.org/10.1016/j.triboint.2015.04.031.

[18] Sharma S, Singh J, Gupta MK, Mia M, Dwivedi SP, Saxena A, et al. Investigation on mechanical, tribological and microstructural properties of Al-Mg-Si-T6/SiC/muscovite-hybrid metal-matrix composites for high strength applications. J Mater Res Technol 2021;12:1564–81. https://doi.org/10.1016/j.jmrt.2021.03.095.

[19] Pragathi P, Elansezhian R. Studies on microstructural and mechanical properties of (Nano SiC+Waste Spent catalyst) reinforced aluminum matrix composites. Mater Today Commun 2022;30:103204. https://doi.org/10.1016/j.mtcomm.2022.103204.

[20] Kumar A, Pal K, Mula S. Effects of cryo-FSP on metallurgical and mechanical properties of stir cast Al7075-SiC nanocomposites. J Alloys Compd 2021;852:156925. https://doi.org/10.1016/j.jallcom.2020.156925.

[21] Krishnan PK, Christy JV, Arunachalam R, Mourad AI, Muraliraja R, Maharbi MA, et al. Production of aluminum alloy-based metal matrix composites using scrap aluminum alloy and waste materials: influence on microstructure and mechanical properties. J Alloys Compd 2019;784:1047–61. https://doi.org/10.1016/j.jallcom.2019.01.115.

[22] Gayathri J, Elansezhian R. Enhancement of mechanical properties of aluminium metal matrix composite by reinforcing waste alumina catalyst and nano Al_2O_3. Mater Today Proc 2021;45:462–6. https://doi.org/10.1016/j.matpr.2020.02.003.
[23] Mazahery A, Shabani MO. Nano-sized silicon carbide reinforced commercial casting aluminum alloy matrix: experimental and novel modeling evaluation. Powder Technol 2012;217:558–65. https://doi.org/10.1016/j.powtec.2011.11.020.
[24] MirHashemi SM, Amadeh A, Khodabakhshi F. Effects of SiC nanoparticles on the dissimilar friction stir weldability of low-density polyethylene (LDPE) and AA7075 aluminum alloy. J Mater Res Technol 2021;13:449–62. https://doi.org/10.1016/j.jmrt.2021.04.094.
[25] Parthiban K, Lakshmanan P, Palani S, Arumugam A. Electroless deposition of SiC Nano Coating on Aluminium alloy and evaluation of wear resistance and electroless characteristics. Mater Today Proc 2021;46:1096–100. https://doi.org/10.1016/j.matpr.2021.01.442.
[26] Donthamsetty S, Babu PS. An ANN approach for predicting the wear behavior of nano SiC-reinforced A356 MMNCs synthesized by ultrasonic-assisted cavitation. Intel Manu Energy Sustain 2021;213:113–24. https://doi.org/10.1007/978-981-33-4443-3_12.
[27] Balasubramanian I, Maheswaran R. Effect of inclusion of SiC particulates on the mechanical resistance behaviour of stir-cast AA6063/SiC composites. Mater Des 2015;65:511–20. https://doi.org/10.1016/j.matdes.2014.09.067.
[28] Liao JH, Yang LX, Chen ZF, Guan TR, Liu TL. Evolution of microstructure and mechanical properties of C_f/SiC-Al composites after high-temperature oxidation. Mater Char 2022;194:112487. https://doi.org/10.1016/j.matchar.2022.112487.
[29] Karthikraja M, Ramanathan K, Loganathan KT, Selvaraj S. Corrosion behaviour of SiC and Al_2O_3 reinforced Al 7075 hybrid aluminium matrix composites by weight loss and electrochemical methods. J Indian Chem Soc 2023;15:101002. https://doi.org/10.1016/j.jics.2023.101002.
[30] Gong D, Zhu M, Cao YF, Qian JR, Chao ZL, Xiu ZY, et al. Revealing the mechanism of internal stress on dimensional stability in SiC/Al composites under long-term thermal exposure. Vacuum 2023;209:111786. https://doi.org/10.1016/j.vacuum.2022.111786.
[31] Cui Y, Wang LF, Ren JY. Multi-functional SiC/Al composites for aerospace applications. Chin J Aeronaut 2008;21:578–84. https://doi.org/10.1016/S1000-9361(08)60177-6.
[32] Sathish T, Sabarirajan N, Saravanan R. Nano-alumina reinforcement on AA 8079 acquired from waste aluminium food containers for altering microhardness and wear resistance. J Mater Res Technol 2021;14:1494–503. https://doi.org/10.1016/j.jmrt.2021.07.041.
[33] Ozdemir I, Ahrens S, Mücklich S, Wielage B. Nanocrystalline Al-Al_2O_3p and SiC_p composites produced by high-energy ball milling. J Mater Process Technol 2008;205:111–8. https://doi.org/10.1016/j.jmatprotec.2007.11.085.
[34] Yigezu BS, Mahapatra MM, Jha PK. On modeling the abrasive wear characteristics of in situ Al-12%Si/TiC composites. Mater Des 2013;50:277–84. https://doi.org/10.1016/j.matdes.2013.02.042.
[35] Attarilar S, Ebrahimi M, Hsieh T-H, Uan J-Y, Göde C. An insight into the vibration-assisted rolling of AA5052 aluminum alloy: tensile strength, deformation microstructure, and texture evolution. Mater Sci Eng A 2021;803:140489. https://doi.org/10.1016/j.msea.2020.140489.
[36] Qing H. 2D micromechanical analysis of SiC/Al metal matrix composites under tensile, shear and combined tensile/shear loads. Mater Des 2013;51:438–47. https://doi.org/10.1016/j.matdes.2013.04.051.
[37] Dinesh Kumar S, Senthamil Selvan T, Sabariraj RV, Muthukumar K, Elayaraja D, Greesan R. Studies on tribological behaviour of AA8050-Si_3N_4 composites. Mater Today Proc 2023;74:68–72. https://doi.org/10.1016/j.matpr.2022.11.144.
[38] Upadhyay NK, Kumaraswamidhas LA, Gahtori B, Muthaiah S, Bathula S, Shyam R, et al. Facile synthesis of earth-abundant and non-toxic p-type $Si_{96}B_4$/SiCp nanocomposites with enhanced thermoelectric performance. Mater Sci Semicond Process 2018;75:234–8. https://doi.org/10.1016/j.mssp.2017.11.039.
[39] Elkady OA, Abolkassema SA, Elsayeda AH, Hussein WA, Hussein KFA. Microwave absorbing efficiency of Al matrix composite reinforced with nano-Ni/SiC particles. Results Phys 2019;12:687–700. https://doi.org/10.1016/j.rinp.2018.11.095.
[40] Manohar G, Pandey KM, Maity SR. Effect of microwave sintering on the microstructure and mechanical properties of AA7075/B_4C/ZrC hybrid nano composite fabricated by powder metallurgy techniques. Ceram Int 2021;47:32610–8. https://doi.org/10.1016/j.ceramint.2021.08.156.
[41] Serajzadeh S, Motlagh SR, Mirbagheri SMH, Akhgar JM. Deformation behavior of AA2017-SiC_p in warm and hot deformation regions. Mater Des 2015;67:318–23. https://doi.org/10.1016/j.matdes.2014.11.042.
[42] Khodabakhshi F, Gerlich AP, Simchi A, Kokabi AH. Hot deformation behavior of an aluminum-matrix hybrid nanocomposite fabricated by friction stir processing. Mater Sci Eng A 2015;626:458–66. https://doi.org/10.1016/j.msea.2014.12.110.
[43] Wang M, Jin P, Wang J, Han L, Cui C. Hot deformation behavior and workability of (SiC_p+$Mg_2B_2O_5$w)/6061 Al hybrid and SiC_p/6061 Al composites. Acta Metall 2014;27:63–74. https://doi.org/10.1007/s40195-014-0023-9.
[44] Jain VKS, Muthukumaran S. Influence of SiC content on microstructure and tribological properties of friction stirprocessed SiC/AA5083 surface composites. Metall Mater Trans A 2019;50:2933–44. https://doi.org/10.1007/s11661-019-05219-8.
[45] Hu JN, Zhu YL, Zhang HT, Li PB, Zhang J, Luo GQ, et al. Interfacial microstructure and sintering mechanism of plasma activated sintered Al/SiC composites. Vacuum 2023;212:112051. https://doi.org/10.1016/j.vacuum.2023.112051.
[46] Bravilin Jiju K, Selvakumar G, Ram Prakash S. Study on preparation of Al – SiC metal matrix composites using powder metallurgy technique and its mechanical properties. Mater Today Proc 2020;27:1843–7. https://doi.org/10.1016/j.matpr.2020.04.001.
[47] Wu HD, Zhang H, Chen S, Fu DF. Flow stress behavior and processing map of extruded 7075Al/SiC particle reinforced composite prepared by spray deposition during hot compression. T Nonferr Metal Soc 2015;25(3):692–8. https://doi.org/10.1016/S1003-6326(15)63654-8.
[48] Mishra D, Nanda AK. Experimental investigation on mechanical properties of stir casted aluminum SiC metal matrix composites. Mater Today Proc 2023;74:1023–7. https://doi.org/10.1016/j.matpr.2022.11.412.
[49] Sharma H, Tiwari SK, Kumar A, Singh D. Investigation of mechanical and erosive behaviour of the Al 6061-SiC composites fabricated by stir casting. Mater Today Proc 2023;69:446–53. https://doi.org/10.1016/j.matpr.2022.09.126.
[50] Kim CS, Cho K, Manjili MH, Nezafati M. Mechanical performance of particulate-reinforced Al metal-matrix composites (MMCs) and Al metal matrix nano-composites

(MMNCs). J Mater Sci 2017;52(23):13319–49. https://doi.org/10.1007/s10853-017-1378-x.
[51] Jiang WM, Zhu JW, Li GY, Guan F, Yu Y, Fan ZT. Enhanced mechanical properties of 6082 aluminum alloy via SiC addition combined with squeeze casting. J Mater Sci Technol 2021;88:119–31. https://doi.org/10.1016/j.jmst.2021.01.077.
[52] Mao DX, Meng XC, Xie YM, Yang YC, Xu YL, Qin ZW, et al. Strength-ductility balance strategy in SiC reinforced aluminum matrix composites via deformation-driven metallurgy. J Alloys Compd 2021;891:162078. https://doi.org/10.1016/j.jallcom.2021.162078.
[53] Huang CJ, List A, Wiehler L, Schulze M, Gartner F, Klassen T. Cold spray deposition of graded Al-SiC composites. Addit Manuf 2022;59:103116. https://doi.org/10.1016/j.addma.2022.103116.
[54] Bastwros M, Kim GY. Ultrasonic spray deposition of SiC nanoparticles for laminate metal composite fabrication. Powder Technol 2016;288:279–85. https://doi.org/10.1016/j.powtec.2015.10.039.
[55] Liu HL, Guo ZY, Yuan XF, Zhu ZW, Gao QQ, Zhang X. Thermoelectric properties of SiC nanocomposite $Mg_2Si_{0.4}Sn_{0.6}$ with Sb doping prepared by vacuum induction levitation melting and spark plasma sintering. Vacuum 2023;213:112135. https://doi.org/10.1016/j.vacuum.2023.112135.
[56] Wang RP, Wang G, Ran SL, Wang W, Zhao Y, Gui KX, et al. Microstructure and mechanical properties of C_f/SiC composite joints joined using $AlCoCrFeNi_{2.1}$ eutectic high-entropy alloy filler via spark plasma sintering. J Eur Ceram Soc 2023;43:1853–63. https://doi.org/10.1016/j.jeurceramsoc.2022.12.045.
[57] Xing Y, Li NY, Li CJ, Gao P, Guan HD, Yang CMY, et al. Effects of size and oxidation treatment for SiC particles on the microstructures and mechanical properties of SiC_p/Al composites prepared by powder metallurgy. Mater Sci Eng 2022;851:143664. https://doi.org/10.1016/j.msea.2022.143664.
[58] Jiao YH, Zhu JF, Ge JL, Shi CJ, Tai YF, Huang YC, et al. Design and fabrication of the ceramic composites via in-situ oxidized process: phase and microstructure evolution in in-situ oxidized SiC/Al–Mg–Si process. Ceram Int 2023;49:1513–20. https://doi.org/10.1016/j.ceramint.2022.10.202.
[59] Wu JQ, Li Z, Wen GY, Gao ZL, Li Y, Zhao YB. Friction mechanism analysis of copper-based composites reinforced with ball-milled and modified composite ceramic powders. Wear 2023;528–529:204959. https://doi.org/10.1016/j.wear.2023.204959.
[60] Dwivedi SP, Saxena A, Sharma S, Singh G, Singh J, Mia M, et al. Effect of ball-milling process parameters on mechanical properties of Al/Al_2O_3/collagen powder composite using statistical approach. J Mater Res Technol 2021;15:2918–32. https://doi.org/10.1016/j.jmrt.2021.09.082.
[61] Mousavian RT, Behnamfard S, Khosroshahi RA, Zavašnik J, Ghosh P, Krishnamurthy S, et al. Strength-ductility trade-off via SiC nanoparticle dispersion in A356 aluminium matrix. Mater Sci Eng 2019;771:138639. https://doi.org/10.1016/j.msea.2019.138639.
[62] Zhang XZ, Chen TJ, Qin H, Wang C. A comparative study on permanent mold cast and powder thixoforming 6061 aluminum alloy and SiC_p/6061Al composite: microstructures and mechanical properties. Materials 2016;9:407. https://doi:10.3390/ma9060407.
[63] Luo YJ, Zhang ZL, Zhou L, Zhang WD, Deng XX, Huang Y, et al. Microstructures and mechanical properties of A356-SiC_p/A356 cladding composite materials prepared by vacuum SolideLiquid casting. J Mater Res Technol 2022;19:4881–9. https://doi.org/10.1016/j.jmrt.2022.07.002.
[64] Shanmuga Priyan VG, Kanmani S. Effect of ultrasonic treatment during stir casting on mechanical properties of AA6063-SiC composites. Mater Chem Phys 2023;294:126977. https://doi.org/10.1016/j.matchemphys.2022.126977.
[65] Devaganesh S, Dinesh Kumar PK, Venkatesh N, Balaj R. Study on the mechanical and tribological performances of hybrid SiC-Al7075 metal matrix composites. J Mater Res Technol 2020;9:3759–66. https://doi.org/10.1016/j.jmrt.2020.02.002.
[66] Ji XH, Li SF, Zhang X, Liu L, Li SL, Gao LN, et al. Influence of characteristic parameters of SiC reinforcements on mechanical properties of AlSi10Mg matrix composites by powder metallurgy. J Mater Res Technol 2023;24:6843–53. https://doi.org/10.1016/j.jmrt.2023.04.262.
[67] Jiang WM, Zhu JW, Li GY, Guan F, Yu Y, Fan ZT. Enhanced mechanical properties of 6082 aluminum alloy via SiC addition combined with squeeze casting. J Mater Sci Technol 2021;88:119–31. https://doi.org/10.1016/j.jmst.2021.01.077.
[68] Mao DX, Meng XC, Xie YM, Yang YC, Xu YL, Qin ZW, et al. Strength-ductility balance strategy in SiC reinforced aluminum matrix composites via deformation-driven metallurgy. J Alloys Compd 2021;891:162078. https://doi.org/10.1016/j.jallcom.2021.162078.
[69] Huang ZY, Xiao BL, Ma ZY. Correlation of hot deformation behaviors and microstructures of 17 vol% SiC_p/Al-Cu-Mg composite fabricated by powder metallurgy. Mater Today Commun 2023;34:105304. https://doi.org/10.1016/j.mtcomm.2022.105304.
[70] Liu SW, Wu HJ, Xie XL, Ji G, Moliere M, Liao HL. Tribological properties of cold-sprayed 7075Al coatings reinforced with hybrid nano-TiB2/micro-SiC particles. Surf Coating Technol 2023;458:129323. https://doi.org/10.1016/j.surfcoat.2023.129323.
[71] Sun MZ, Guo HL, Zheng JL, Wang Y, Liu XH, Li Q, et al. Hydrophobic octadecylamine-polyphenol film coated slow released urea via one-step spraying co-deposition. Polym Test 2023;91:106831. https://doi.org/10.1016/j.polymertesting.2020.106831.
[72] Elansezhian R, Ramamoorthy B, Nair PK. Effect of surfactants on the mechanical properties of electroless (Ni-P) coating. Surf Coating Technol 2008;203:709–12. https://doi.org/10.1016/j.surfcoat.2008.08.021.
[73] Thirugnanasambandam A, Selvakumaran T, Subbiah R, Ramachandran K, Manickam S. Development of high-performance aluminium 6061/SiC nanocomposites by ultrasonic aided rheo-squeeze casting method. Ultrason Sonochem 2021;76:105631. https://doi.org/10.1016/j.ultsonch.2021.105631.
[74] Arunkumar T, Pavanan V, Murugesan VA, Mohanavel V, Ramachandran K. Influence of nanoparticles reinforcements on Al 6061 alloys fabricated via novel ultrasonic aided rheo-squeeze casting method. Met Mater Int 2022;28:145–54. https://doi.org/10.1007/s12540-021-01036-0.
[75] Wan BB, Liu YT, Chen WP, Lu TW, Jin SX, Xu X, et al. Effect of reinforcement types on the ball milling behavior and mechanical properties of 2024Al matrix composites. J Mater Res Technol 2023;23:268–83. https://doi.org/10.1016/j.jmrt.2023.01.024.
[76] Zhang ZH, Wang FC, Luo J, Lee SK, Wang L. Microstructures and mechanical properties of spark plasma sintered Al–SiC composites containing high volume fraction of SiC. Mater Sci Eng 2010;527:7235–40. https://doi:10.1016/j.msea.2010.07.043.
[77] Leszczyńska-Madeja B, Garbiecb D, Madej M. Effect of sintering temperature on microstructure and selected properties of spark plasma sintered Al-SiC composites.

Vacuum 2019;164:250–5. https://doi.org/10.1016/j.vacuum.2019.03.033.
[78] Zare R, Sharifi H, Saeri MR, Tayebi M. Investigating the effect of SiC partciles on the physical and thermal properties of Al6061/SiC composites. J Alloys Compd 2019;801:520–8. https://doi.org/10.1016/j.jallcom.2019.05.317.
[80] Rawat A, Kumar A, Agrawal AP. Investigation of mechanical properties of heat-treated A356/SiC composite fabricated through stir casting technique. Mater Today Proc 2022;62:203–8. https://doi.org/10.1016/j.matpr.2022.02.618.
[81] Ashok N, Johnson Santhosh A, Tura AD, Mamo HB, Lemma EA, Melaku LE. Effect of stirring speed and time on the mechanical properties of Al8011-SiC metal matrix composites. Mater Today Proc 2022;64:194–9. https://doi.org/10.1016/j.matpr.2022.04.364.
[82] Wu CC, Gao T, Nie JF, Jiang L, Liu XF. In-situ synthesis of nano SiC particles in Al-Si-C system at 750°C. J Mater Res Technol 2021;13:716–26. https://doi.org/10.1016/j.jmrt.2021.05.008.
[83] Jiang JF, Wang Y. Microstructure and mechanical properties of the semisolid slurries and rheoformed component of nano-sized SiC/7075 aluminum matrix composite prepared by ultrasonic-assisted semisolid stirring. Mater Sci Eng 2015;639:350–8. https://doi.org/10.1016/j.msea.2015.04.064.
[84] Li JY, Lv SL, Wu SS, Zhao DJ, Li F, Guo W. Effects of nanoparticles on the solution treatment and mechanical properties of nano-SiC_p/Al-Cu composites. J Mater Process Technol 2021;296:117195. https://doi.org/10.1016/j.jmatprotec.2021.117195.
[85] Shokrieh MM, Moshrefzadeh-Sani H. On the constant parameters of Halpin-Tsai equation. Polymer 2016;106:1–20. https://doi.org/10.1016/j.polymer.2016.10.049.
[86] Hosseinzadeh A, Yapici GG. High temperature characteristics of Al2024/SiC metal matrix composite fabricated by friction stir processing. Mater Sci Eng 2018;731:487–94. https://doi.org/10.1016/j.msea.2018.06.077.
[87] Song YF, Ding XF, Zhao XJ, Xiao LR, Yu CX. The effect of SiC addition on the dimensional stability of Al-Cu-Mg alloy. J Alloys Compd 2018;750:111–6. https://doi.org/10.1016/j.jallcom.2018.03.257.
[88] Thimmarayan R, Thanigaiyarasu G. Effect of particle size, forging and ageing on the mechanical fatigue characteristics of Al6082/SiC_p metal matrix composites. Int J Adv Manuf Technol 2010;48:625–32. https://doi.org/10.1007/s00170-009-2316-0.
[89] Jiang JF, Chen G, Wang Y. Compression mechanical behavior of 7075 aluminum matrix composite reinforced with nano-sized SiC particles in semisolid state. J Mater Sci Technol 2016;32:1197–203. https://doi.org/10.1016/j.jmst.2016.01.015.
[90] Zhao ZD, Chen Q, Wang YB, Shu DY. Microstructural evolution of an ECAE-formed ZK60-RE magnesium alloy in the semi-solid state. Mater Sci Eng 2009;506:8–15. https://doi.org/10.1016/j.msea.2008.12.042.
[91] Huang SJ, Ali AN. Experimental investigations of effects of SiC contents and severe plastic deformation on the microstructure and mechanical properties of SiC_p/AZ61 magnesium metal matrix composites. J Mater Process Technol 2019;272:28–39. https://doi.org/10.1016/j.jmatprotec.2019.05.002.
[92] Peng C, Cao GW, Gu TZ, Wang C, Wang ZY, Sun C. The effect of dry/wet ratios on the corrosion process of the 6061 Al alloy in simulated Nansha marine atmosphere. Corrosion Sci 2023;210:110840. https://doi.org/10.1016/j.corsci.2022.110840.
[93] Ravi Kumar M, Reddappa HN, Suresh R, Gangadharappa M. Effect of heat treatment on tensile strength of Al7075/Al_2O_3/SiC_p hybrid composite by stir casting technique. Mater Today Proc 2018;5:22460–5. https://doi.org/10.1016/j.matpr.2018.06.616.
[94] Parameshwaranpillai T, Lakshminarayanan PR, Nageswara Rao B. Tensile fracture strength of 2124Al–10 vol.% SiC_p composite compact tension specimens. Mater Des 2010;31:2987–93. https://doi.org/10.1016/j.matdes.2010.01.032.
[95] Wu H, Xu WC, Shan DB, Wang XJ, Guo B, Jin BC. Micromechanical modeling of damage evolution and fracture behavior in particle reinforced metal matrix composites based on the conventional theory of mechanism-based strain gradient plasticity. J Mater Res Technol 2023;22:625–41. https://doi.org/10.1016/j.jmrt.2022.11.139.
[96] Zhang Y, Shen R, Li M, Pang J, Zhang L, Li S, et al. Mechanical damage behavior of metal matrix composites with the arbitrary morphology of particles. J Mater Res Technol 2020;9:7002–12. https://doi.org/10.1016/j.jmrt.2020.05.014.
[97] Sun W, Duan CZ, Yin WD. Development of a dynamic constitutive model with particle damage and thermal softening for Al/SiC_p composites. Compos Struct 2020;236:111856. https://doi.org/10.1016/j.compstruct.2020.111856.
[98] Li DX, Hu KQ, Han MX, Xie KW, Liu GL, Liu XF. Strength adjust mechanism of high toughness Al_4C_3/Al-xMg composites. Mater Sci Eng 2021;824:141842. https://doi.org/10.1016/j.msea.2021.141842.
[99] Xue C, Yu JK. Enhanced thermal transfer and bending strength of SiC/Al composite with controlled interfacial reaction. Mater Des 2014;53:74–8. https://doi.org/10.1016/j.matdes.2013.06.056.
[100] Yamamoto M, Nishimura Y, Hayashida M. Influence of Al particles as infiltration promoters on the interfacial reaction and mechanical property of a continuous SiC fiber/AZ91 composite fabricated by a low-pressure infiltration method. J Alloys Compd 2021;887:161461. https://doi.org/10.1016/j.jallcom.2021.161461.
[101] Tong HT, Zuo R, Qiu D, Li X, Qiu F. Interfacial reaction behavior and evolution mechanism at a preoxidized SiC_{ox}/Al interface. J Mater Res Technol 2021;15:1100–14. https://doi.org/10.1016/j.jmrt.2021.08.003.
[102] Vashisth A, Mirsayar MM. A combined atomistic-continuum study on the temperature effects on interfacial fracture in SiC/SiO_2 composites. Theor Appl Fract Mech 2020;105:102399. https://doi.org/10.1016/j.tafmec.2019.102399.
[103] Gecü R, Karaaslan A. Volume fraction effect of stainless steel on microstructure, interface, corrosion and wear behavior of stainless steel/aluminum bimetal composites. Mater Chem Phys 2022;284:126068. https://doi.org/10.1016/j.matchemphys.2022.126068.
[104] Kumar J, Singh D, Kalsi NS, Sharma S, Pruncu CI, Pimenov DY, et al. Comparative study on the mechanical, tribological, morphological and structural properties of vortex casting processed, Al–SiC–Cr hybrid metal matrix composites for high strength wear-resistant applications: fabrication and characterizations. J Mater Res Technol 2020;9:13607–15. https://doi.org/10.1016/j.jmrt.2020.10.001.
[105] Gopalakannan S, Senthilvelan T. Application of response surface method on machining of Al–SiC nano-composites. Measurement 2013;46:2705–15. https://doi.org/10.1016/j.measurement.2013.04.036.
[106] Wu C, Fang XD, Kang Q, Fang ZY, Sun H, Zhang D, et al. Formation mechanism, interface characteristics and the

application of metal/SiC thin-film ohmic contact after high-temperature treatment. J Mater Res Technol 2023;24:2428–41. https://doi.org/10.1016/j.jmrt.2023.03.117.
[107] Wright NG, Horsfall AB, Vassilevski K. Prospects for SiC electronics and sensors. Mater Today 2008;11:16–21. https://doi.org/10.1016/S1369-7021(07)70348-6.
[108] Fraga MA, Pessoa RS, Massi M, Maciel HS. Silicon carbide as base material for MEMS sensors of aerospace use: an overview. Materia 2014;19(3):274–90. https://doi.org/10.1590/S1517-70762014000300011.
[109] Lee H, Sohn SS, Jeon C, Jo I, Lee S-K, Lee S. Dynamic compressive deformation behavior of SiC-particulate-reinforced A356 Al alloy matrix composites fabricated by liquid pressing process. Mater Sci Eng 2017;680:368–77. https://doi.org/10.1016/j.msea.2016.10.102.
[110] Zhang YW, liu WK, Gui ZW, Zhou SH, Ren ZD. Damage mechanisms of 2.5D SiO_{2f}/SiO_2 woven ceramic matrix composites under compressive impact. Ceram Int 2023;49:9203–18. https://doi.org/10.1016/j.ceramint.2022.11.083.
[113] Pezzotti G, Müller WH. Strengthening mechanisms in Al_2O_3/SiC nanocomposites. Comput Mater Sci 2001;22:155–68. https://doi.org/10.1016/S0927-0256(01)00185-9.
[114] Hasan ST, Beynon JH, Faulkner RG. Role of segregation and precipitates on interfacial strengthening mechanisms in SiC reinforced aluminium alloy when subjected to thermomechanical processing. J Mater Process Technol 2004;153–154:758–64. https://doi.org/10.1016/j.jmatprotec.2004.04.183.
[115] Silvestroni L, Corradetti S, Manzolaro M, Mi Ballan, Cesarotto D, Sciti D, et al. Novel SiC/C composite targets for the production of radioisotopes for nuclear applications. J Eur Ceram Soc 2022;42:6750–6. https://doi.org/10.1016/j.jeurceramsoc.2022.07.017.
[116] Pellegrini C, Balat-Pichelin M, Rapaud O, Bêche E. Oxidation resistance of Zr- and Hf-diboride composites containing SiC in air plasma up to 2600K for aerospace applications. Ceram Int 2022;48:2177–90. https://doi.org/10.1016/j.ceramint.2021.09.310.
[117] Sharma S, Singh J, Gupta MK, Mia M, Dwivedi SP, Saxena A, et al. Investigation on mechanical, tribological and microstructural properties of Al-Mg-Si-T6/SiC/muscovite-hybrid metal-matrix composites for high strength applications. J Mater Res Technol 2021;12:1564–81. https://doi.org/10.1016/j.jmrt.2021.03.095.
[118] Gevorkyan ES, Rucki M, Kagramanyan AA, Nerubatskiy VP. Composite material for instrumental applications based on micro powder Al_2O3 with additives nano-powder SiC. Int J Refract Met Hard Mater 2019;82:336–9. https://doi.org/10.1016/j.ijrmhm.2019.05.010.
[119] Lin ZC, Su YS, Qiu CH, Yang JY, Chai XS, Liu XY, et al. Configuration effect and mechanical behavior of particle reinforced aluminum matrix composites. Scripta Mater 2023;224:115135. https://doi.org/10.1016/j.scriptamat.2022.115135.
[120] Ma SM, Shang ZX, Shang AY, Zhang P, Tang CL, Huang YZ, et al. Additive manufacturing enabled synergetic strengthening of bimodal reinforcing particles for aluminum matrix composites. Addit Manuf 2023;6:103543. https://doi.org/10.1016/j.addma.2023.103543.
[121] Guan HD, Li CJ, Gao P, Prashanth KG, Tan J, Eckert J, et al. Aluminum matrix composites reinforced with metallic glass particles with core-shell structure. Mater Sci Eng 2020;771:138630. https://doi.org/10.1016/j.msea.2019.138630.
[122] Ansary Yar A, Montazerian M. Microstructure and mechanical properties of aluminum alloy matrix composite reinforced with nano-particle MgO. J Alloys Compd 2009;484:400–4. https://doi.org/10.1016/j.jallcom.2009.04.117.
[123] Zhang ZG, Zhao GF, Han B, Zhong JW, Xie J. SiC-foam structured Ni-based catalyst derived from perovskites for methane value-added application: enhanced resistance to Ni sintering and stability. Mol Catal 2021;513:111831. https://doi.org/10.1016/j.mcat.2021.111831.
[124] Chen ZD, Wu ZY, Su JJ, Li JP, Gao B, Fu JJ, et al. Large-scale and low-cost synthesis of in situ generated SiC/C nano-composites from rice husks for advanced electromagnetic wave absorption applications. Surf Coating Technol 2021;406:126641. https://doi.org/10.1016/j.surfcoat.2020.126641.
[125] Wang H, Li ZY, Shang Z, Tian LM. Preparation of porous SiC ceramics skeleton with low-cost and controllable gradient based on liquid crystal display 3D printing. J Eur Ceram Soc 2022;42:5432–7. https://doi.org/10.1016/j.jeurceramsoc.2022.07.002.
[126] Tang J, Liu M, Wei YQ, Yang Y, Huang ZR. An efficient and low-cost liquid silicon infiltration method to prepare SiC-coated carbon short fiber for fiber protection of Cf/SiC ceramic matrix composites. Ceram Int 2021;47:13235–41. https://doi.org/10.1016/j.ceramint.2021.01.115.
[127] Xu M, Girish YR, Rakesh KP, Wu P, Manukumar HM, Byrappa SM, et al. Recent advances and challenges in silicon carbide (SiC) ceramic nanoarchitectures and their applications. Mater Today Commun 2021;28:102533. https://doi.org/10.1016/j.mtcomm.2021.102533.
[128] Mazahery A, Shabani MO. Nano-sized silicon carbide reinforced commercial casting aluminum alloy matrix: experimental and novel modeling evaluation. Powder Technol 2012;217:558–65. https://doi.org/10.1016/j.powtec.2011.11.020.
[129] Raghavendra C, Basavarajappa S, Sogalad I, Kumar S. A review on Ni based nano composite coatings. Mater Today Proc 2021;39:6–16. https://doi.org/10.1016/j.matpr.2020.04.810.
[130] Liang Y, Li YS, Yu QY, Zhang YX, Zhao WJ, Zeng ZX. Structure and wear resistance of high hardness Ni-B coatings as alternative for Cr coatings. Surf Coating Technol 2015;264:80–6. https://doi.org/10.1016/j.surfcoat.2015.01.016.
[131] Prasad B. Investigation into sliding wear performance of zinc-based alloy reinforced with SiC particles in dry and lubricated conditions. Wear 2007;262:262–73. https://doi.org/10.1016/j.wear.2006.05.004.
[132] Ezatpour HR, Parizi MT, Sajjadi SA, Ebrahimi GR, Chaichi A. Microstructure, mechanical analysis and optimal selection of 7075 aluminum alloy based composite reinforced with alumina nanoparticles. Mater Chem Phys 2016;178:119–27. https://doi.org/10.1016/j.matchemphys.2016.04.078.
[133] Xiao Y, Li DS, Qian Z, Li Y. An experimental and numerical study of curing deformation considering tool-part interaction for two-step curing tooling composite materials. J Manuf Process 2023;94:435–53. https://doi.org/10.1016/j.jmapro.2023.03.069.
[134] Liu JB, Zhao XQ, Yang Q, Wang K, Fu YF, Yang QL. Particle-reinforced ultralight hollow Ni-P-B4C microlattice composite materials. Mater Lett 2023;331:133438. https://doi.org/10.1016/j.matlet.2022.133438.

FURTHER READING

[79] Farrokhzad M, Khan T. Sliding wear performance of nickel-based cermet coatings composed of WC and Al_2O_3 nanosized

particles. Surf Coating Technol 2016;304:401–12. https://doi.org/10.1016/j.surfcoat.2016.07.014.

[111] AbuShanab WS, Moustafa EB. Effects of friction stir processing parameters on the wear resistance and mechanical properties of fabricated metal matrix nanocomposites (MMNCs) surface. J Mater Res Technol 2020;9:7460–71. https://doi.org/10.1016/j.jmrt.2020.04.073.

[112] Bembalge OB, Panigrahi SK. Development and strengthening mechanisms of bulk ultrafine grained AA6063/SiC composite sheets with varying reinforcement size ranging from nano to micro domain. J Alloys Compd 2018;766:355–72. https://doi.org/10.1016/j.jallcom.2018.06.306.

Dr. Yunlei Wang, an Assistant Professor of Materials Engineering at Chongqing University of Arts and Sciences, Chongqing, is will be engaged in postdoctoral research at the University of Napoli Federico II, Italy. He received his Ph.D. degree in 2017 from the Materials Sciences and Engineering of Chongqing University. Yunlei is the author of more than 20 papers published in international journals, and more than 30 scientific research projects have been obtained. He interested in the studies of materials fabrication, microstructures and properties analysis for light alloy, film materials, composite materials, nanomaterials. In the current studies, he focus on the characterization of the microstructures and properties through the methods of OM, SEM, EBSD, XRD and TEM.

Prof. Tullio Monetta, a Professor in Department of Chemical Engineering, Materials and Industrial Production, University of Napoli Federico II, Italy. He received his Ph.D. from Department of chemical engineering, materials and industrial production of University of Napoli Federico II in 1993, Italy. He deeply involved in aluminum characterization and surface treatments as well as light metal studies, and interested in corrosion, coatings, titanium, aluminum, magnesium, graphene, polydopamine, and other aspects. In a word, a deep understanding of the microstructure and properties of metal materials was established. Prof. Tullio Monetta, who has published more than 100 papers in international journals.